12-2014

A step towards understanding of the molecular basis of ligand promiscuity in the aminoglycoside modifying enzymes

Sherin R. Raval
University of Tennessee - Knoxville, sraval@vols.utk.edu

To the Graduate Council:

I am submitting herewith a thesis written by Sherin R. Raval entitled "A step towards understanding of the molecular basis of ligand promiscuity in the aminoglycoside modifying enzymes." I have examined the final electronic copy of this thesis for form and content and recommend that it be accepted in partial fulfillment of the requirements for the degree of Master of Science, with a major in Biochemistry and Cellular and Molecular Biology.

Engin H. Serpersu, Major Professor

We have read this thesis and recommend its acceptance:

Gladys Alexandre, Hong Guo

Accepted for the Council:
Carolyn R. Hodges

Vice Provost and Dean of the Graduate School

(Original signatures are on file with official student records.)

A step towards understanding of the molecular basis of ligand promiscuity in the aminoglycoside modifying enzymes

A Thesis Presented for the
Master of Science
Degree
The University of Tennessee, Knoxville

Sherin R. Raval

December 2014

DEDICATED

To my parents:

Hema R. Raval

And

Ramesh C. Raval

To my brother:

Karan R. Raval

ACKNOWLEDGEMENTS

I am utterly grateful to my parents for their consistent love and encouragement. I am also thankful to them for providing me with the courage to live up to my dreams. I thank my brother Karan Raval for his witty sense of humor and being a strong pillar of support and joy. I would not be here without you!

I would like to thank my mentor Dr. Engin H. Serpersu for his guidance and patience throughout this project. I would also like to thank Dr. Gladys Alexandre and Dr. Hong Guo for their suggestions and interest in this project.

I would like to thank Dr. Gretchen L. Anderson for sparking my interest in biochemistry. Finally, I thank all my friends for being there for me throughout!

ABSTRACT

Aminoglycosides have proven very useful in the treatment of infections; lately their effectiveness has been greatly reduced due to increasing resistance. Among many known mechanisms of resistance to aminoglycosides, enzymatic modification is the most prevailing. More than 14 aminoglycoside -*N3*-acetyltransferases- a class of aminoglycoside modifying enzymes, are known today. This study focuses on a pair of acetyl transferases: The aminoglycoside-*N3*- acetyltransferase IIIb (AAC-IIIb) and the aminoglycoside-*N3*-acetyltransferase IIa (AAC-IIa). AAC-IIa and AAC-IIIb are very similar in their amino acid sequence and structure – yet they have a strong difference in their substrate selectivity, kinetic and thermodynamic properties. This work represents a comparative study of these two enzymes in an effort to determine thermodynamic basis of the differential substrate profiles of AAC-IIa to AAC-IIIb.

Table of Contents

LIST OF TABLES

LIST OF FIGURES

LIST OF ABBREVIATIONS

AAC-IIa: Aminoglycoside Acetyltransferase (3)-IIa

AAC-IIIb: Aminoglycoside Acetyltransferase (3)-IIIb

ANT (4'): Aminoglycoside Nucleotidyltransferase (4')

APH (3')-IIIa: Aminoglycoside Phosphotransferase (3')-IIIa

AACs : Aminoglycoside N-acetyltransferases

AcCoA: Acetyl Coenzyme A

AGME: Aminoglycoside Modifying Enzyme

CoASH: Coenzyme A

Δ: delta (change in…)

°C: Degree Celcius

T_m: Melting temperature

2-DOS: 2-deoxystreptamine

DTT: Dithiothreitol

GNAT: GCN5 related acetyltransferase

HSQC: Heteronuclear Single Quantum Coherence

IPTG: Isopropyl β-D-1-thiogalactopyranoside

ITC: Isothermal Titration Calorimetry

NMR: Nuclear Magnetic Resonance

DSC: Differential Scanning Calorimetry

CD: Circular Dichroism

AUC: Analytical Ultra centrifugation

PMSF: phenylmethanesulphonylfluoride

Tris-HCl: 2-Amino-2-hydroxymethyl-propane-1, 3-diol hydrochloride

BLAST: Basic Local Alignment Search Tool

MOPS: 3-(N-morpholino) propanesulfonic acid

NaCl: Sodium chloride

Chapter 1: Introduction

I. Aminoglycoside Antibiotics:

i. History:

An aminoglycoside is a molecule composed of amino modified sugars. Aminoglycoside antibiotics are traditional therapeutic agents against gram negative bacterial strains and a few anaerobic bacilli [1]. Streptomycin was the first of this kind of antibiotics to be used to treat tuberculosis after its discovery in 1941. Aminoglycoside antibiotics do have potent side effects such as nausea, fatigue, anaphylactic shock, ototoxicity and nephrotoxicity, justifying for their use to be carefully monitored [2, 3]. In the United States the U.S. Food and Drug Administration has approved streptomycin, neomycin, gentamycin, tobramycin, amikacin and paramomycin for clinical use [4]. In combination with other anti-bacterials, aminoglycoside antibiotics are also used to treat gram-positive infections. They have also been shown to be effective to treat protozoan and mycobacterial infections as well as some genetic diseases, cystic fibrosis and inhibition of the HIV virus reproduction [5]. The extensive use of these antibiotics is due to their diverse chemical structures, origins and availability [6]. Aminoglycoside antibiotics, just like other classes of antibiotics, are a group of antimicrobial compounds currently experiencing reduced efficiency in fighting bacterial infections, due to growing bacterial resistance against them.

ii. Nomenclature and Classification:

Most aminoglycoside antibiotics originate from either bacteria or fungi, unless they are synthetic. The general nomenclature of antibiotics are such that those derived from the bacteria of the *Streptomyces* genus are named with a suffix of 'mycin' and the ones from the fungus *Micromonospora* are named with a suffix 'micin' [7]. Penicillin is derived from *Penicillium* fungi whereas Streptomycin is derived from the actinobacterium *Streptomyces griseus* [8]. However, the façade of the suffixes does not suggest common mechanism of action. For instance, vancomycin, a glycopeptide antibiotic binds to the amino acids within the cell wall thereby inhibiting cell wall synthesis while paromomycin binds to the 16S ribosomal RNA and inhibits protein synthesis. In contrast, erythromycin, a macrolide inhibits protein synthesis by preventing the activity of the peptidyltransferase that forms peptide bonds between adjacent amino acids during protein synthesis [9-11].

The majority of aminoglycoside antibiotics can be classified into two major categories: the neomycin family and the kanamycin family. They have a common 2-deoxystreptamine (2-DOS) ring that is linked by glycosidic bonds to the amino sugars [3] ,as shown in Figure 1. As noted in the kanamycin structure, rings A, B, and C are referred to as the primed, unprimed and double primed rings, respectively. The kanamycin family of aminoglycosides have a 4,6-disubstituted central deoxystreptamine ring while the ones belonging to the neomycin family have a 4,5-disubstituted central deoxystreptamine ring [12]. Addition of methyl, amino and hydroxyl groups and of

sugar rings, are a few of the many modifications found to occur on the chemical backbone of these two groups of aminoglycosides

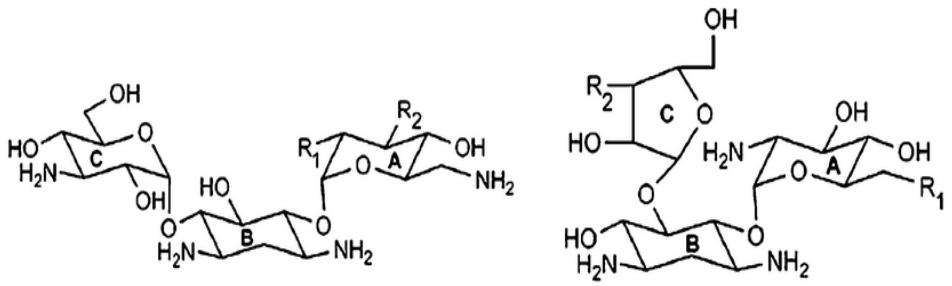

	R_1	R_2		R_1	R_2
Kanamycin A	OH	OH	Ribostamycin	NH_2	OH
Kanamycin B	NH_2	OH	Neomycin	NH_2	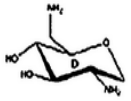
Tobramycin	NH_2	H	paromomycin	OH	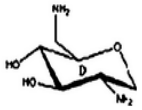

Figure 1: Structures of few aminoglycoside antibiotics - (L) Kanamycin family (R) Neomycin family. Figure reprinted with permission from Ozen, C., et al., *Detection of specific solvent rearrangement regions of an enzyme: NMR and ITC studies with aminoglycoside phosphotransferase (3')-IIIa.* Biochemistry, 2008. 47(1): p. 40-9. Copyright © 2008, American Chemical Society.

iii. Mode of Action:

Early studies to understand the mechanism of aminoglycosides antibacterial action showed that they caused miscoding during the protein synthesis, leading to low cell

sustainability and improper cell wall formation, and eventually, cell death [13]. Due to their protonated amine moieties they have a high binding affinity to the RNAs, especially to the prokaryotic rRNA that is 10 fold higher as compared to the eukaryotic rRNA [14, 15]. They are known to bind the tRNA, the Rev response element (RRE) for transcriptional activation region in human immunodeficiency virus (HIV), the hammerhead ribozyme, group I self-splicing introns and the ribozyme from the hepatitis delta virus [16]. Other studies discovered that the aminoglycosides bind to the amino-acyl-tRNA decoding site (A-site) on the 16S RNA subunit of the ribosome [15]. Crystal structure shows that when the free 30S ribosomal subunit is unbound there is a loop on the A-site in which two adenines are folded back inside the helix. At the A-site, the matching of correct anticodon to the codon of the mRNA is done during translation. Upon accurate matching, these two adenines are unfolded from the helix and translation occurs [17-19]. One crystallography study has shown that upon binding of the aminoglycoside paromomycin to the 30S ribosomal unit, the primed ring of the aminoglycoside was inserted inside the helix, forcing the two adenines out of the helix. The central unprimed ring also shows interaction with many conserved base pairs of the A-site [16]. Hence, the primed and unprimed rings of the aminoglycosides hinder the process of translation by binding to the conserved regions of the 16S rRNA, causing mistranslations and premature stops in protein synthesis, resulting in cell death. Later, studies from our research group demonstrated that the primed and unprimed rings of aminoglycosides adopt a similar conformation when bound to aminoglycoside modifying enzymes and make the most significant interactions with these enzymes [20].

iv. Antibiotic Resistance:

Antibiotics are a wonderful invention for curing infections caused by bacteria. Unfortunately bacteria are adept at developing resistance against them. Upon over exposure to the same antibiotics, bacterial population becomes available to develop the ability to modify these drugs to alleviate their toxic effect. Examples of such modification of antibiotics include a change in the structure of the drug, inactivating or neutralizing its effect [7]. Bacteria are also able to transfer genes coding for antibiotic resistance, rapidly spreading resistance to a particular antibiotic [6]. This issue is amplified when the antibiotics are used to treat infections against which they are not effective or as preventative measure, instead of treatment. Resistance to antibiotics poses a serious problem, as an increasing number of infections can no longer be treated with existing medications.

II. Aminoglycoside Modifying Enzymes:

i. Classification, peculiarities and significance:

Aminoglycosides are a broad group of antibiotics that are produced by *actinomycetes* as a defense mechanism against other bacteria [1, 12]. In order to overcome the effects of antibiotics, bacteria also produce enzymes that modify aminoglycosides to mediate antibiotic resistance and render them harmless [3]. To date, from both gram-positive and gram-negative bacteria, there are more than 50 known enzymes that modify aminoglycoside. These enzymes are known as the aminoglycoside modifying enzymes (AGMEs) [21]. AGMEs are divided in classes based on the chemical group they transform [22]. The three major classes of AGMEs are; the acetyltransferases (AACs) -catalyze the acetyl CoA-dependent acetlylation of an amino group, the nucleotidyltransferases (ANTs) - catalyze ATP-dependent adenylation of hydroxyl groups and the phosphotransferases (APHs) - catalyze ATP-dependent phosphorylation of a hydroxyl group. AGMEs are further characterized by the location of the modification that they enable. For example aminoglycoside phosphotransferase 3' type IIIa (APH (3')-IIIa) phosphorylates the hydroxyl attached to the C-3 on the primed ring of the aminoglycoside antibiotic[23]. Various modification sites of AGMEs are shown on a Kanamycin family aminoglycoside antibiotic in Figure 2. Because different AGME may catalyze similar chemical modifications, these AGME are further characterized by discovery and resistance profile [24]. Within each family of AGME transferases, substrate promiscuity varies, i.e. many enzymes are able to modify

several structurally diverse aminoglycoside antibiotics and are not specific to just a single aminoglycoside.

Modifications to aminoglycosides by catalytic action of AGMEs reduces the binding affinity of aminoglycosides for the A site of the 30S RNA subunit by creating unfavorable electrostatic interactions and steric hindrance. To simplify, when a negatively charged phosphate group is added, it changes the attraction of the aminoglycoside to the negatively charged A-site [16]. Chemical modifications at different sites on aminoglycosides decrease their binding affinity for the A-site to varying degrees. Further, bacterial strains are likely to produce several aminoglycoside modifying enzymes [25]. The study of these enzymes is thus not only relevant to the treatment of infections but also can be of immense help for future drug design and development. Apart from clinical interest, analysis of AGME and its substrates gives insights into the understanding of protein-ligand interactions, as many of these enzymes interact with various aminoglycoside antibiotics. This can also help to explain "dynamics", which measures the nature and degree of fluctuations in the protein structure in presence and absence of ligands. Understanding molecular basis of "promiscuity" to determine reasons for interaction with a wide set of substrates for a protein are also studied using this family of enzymes.

The AGMEs are often characterized in terms of promiscuity. If the AGME can bind a large number of substrates, it is considered promiscuous while the ones that can bind to only few substrates have low promiscuity. In this work, we define an AGME to be promiscuous if it can bind to two or more classes of aminoglycosides. For instance, the aminoglycoside phosphotransferase-IIIa, APH (3')-IIIa, can modify over 15 aminoglycosides

from the kanamycin and neomycin families. APH (3')-IIIa is qualified as highly promiscuous in this work. While an acetyl transferase, AAC (3)-IIa can only modify several members of kanamycins, it is unable to modify neomycins at an appreciable rate and it is qualified as having a moderately low promiscuity. On the other hand, the aminoglycoside acetyltransferase (3)-VIa only modifies 3 members of the kanamycins, which represents a limited substrate profile. Sequence comparison of AGMEs showed that neither promiscuity nor substrate overlap could be deduced from amino acid sequence analysis. For example, AGMEs with less than 10% sequence similarity can have a large substrate overlap. Conversely, enzymes with sequence similarity of 50-60% may have non-overlapping substrate profiles. The same conclusion can be made regarding their substrate promiscuity. [21].

To date, several AGMEs have been studied using kinetic, biochemical and biophysical techniques [26, 27]. Several crystal structures of AGMEs are also available, with or without bound substrates [27-31]. However, the molecular basis for the discrepancy in substrate specificity between these enzymes remains unidentified.

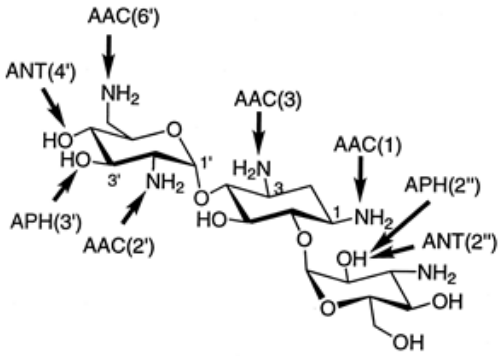

Figure 2: Various AGME modification sites shown on aminoglycoside antibiotic Kanamycin B

Chapter 2: The Two Acetyl Transferases - So Alike Yet So Different!

I. The Aminoglycoside *N*-Acetyltransferases

i. Overview:

Inactivation by AGMEs is one of the most prevalent mechanisms used by bacteria to create resistance to the aminoglycoside antibiotics. One such class of AGMEs is the aminoglycoside N-acetyltransferases (AACs). AACs belong to the GCN5-related N-acetyltransferase (GNAT) superfamily that consists of over 10,000 proteins [32]. The GNAT enzymes use acetyl coenzyme A as a donor substrate to catalyze the acetylation of the $–NH_2$ groups in the acceptor molecule. Crystal structures of several acetyltransferases have been resolved along with extensive study of its mechanical and structural aspects [33-35]. Depending on the position of the $–NH_2$ modified by the AACs by acetylation, these enzymes are further classified as AAC (1), AAC (3), AAC (2') and AAC (6') [25].

This work focuses on two AAC (3) enzymes that catalyze the transfer of an acetyl coenzyme A (AcCoA) to the amine groups at the C3 position of the aminoglycosides. This reaction is shown in the Figure 3 below.

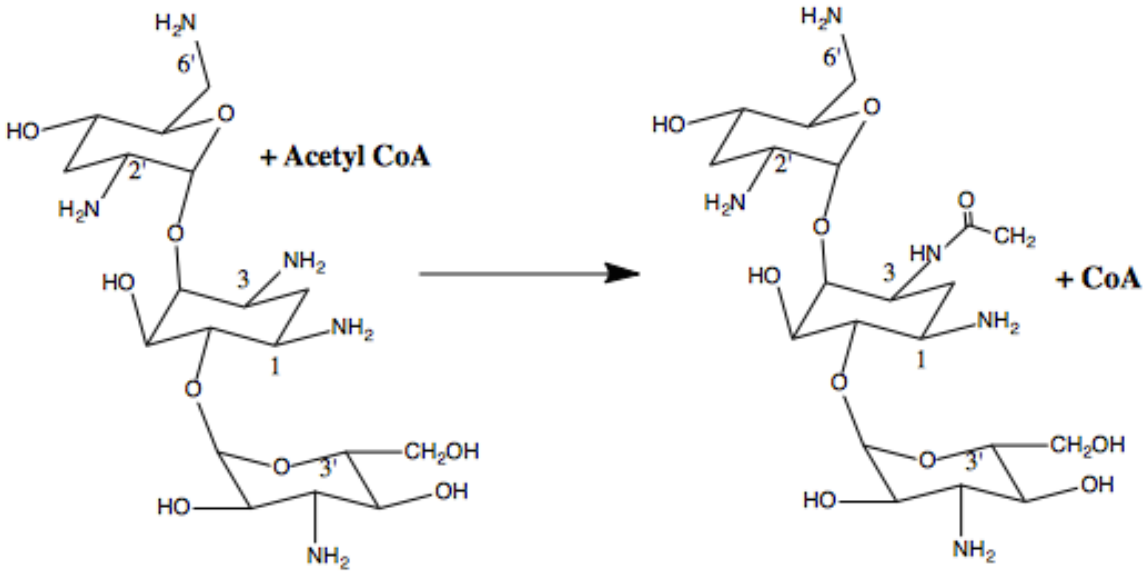

Figure 3: Acetylation of the aminoglycoside Tobramycin via AAC (3).

The substrate profile and promiscuity of various AAC (3) enzymes vary. This work focuses on a low promiscuity protein, the aminoglycoside *N3* acetyltransferase IIa (AAC-IIa) and compares it to the aminoglycoside *N3* acetyl transferase IIIb (AAC-IIIb), APH (3')-IIIa and to an aminoglycoside nucleotidyltransferase, (4') (ANT), previously characterized by our research group. The substrates used throughout this study are the aminoglycoside tobramycin and the cofactor CoASH (Figure 5).

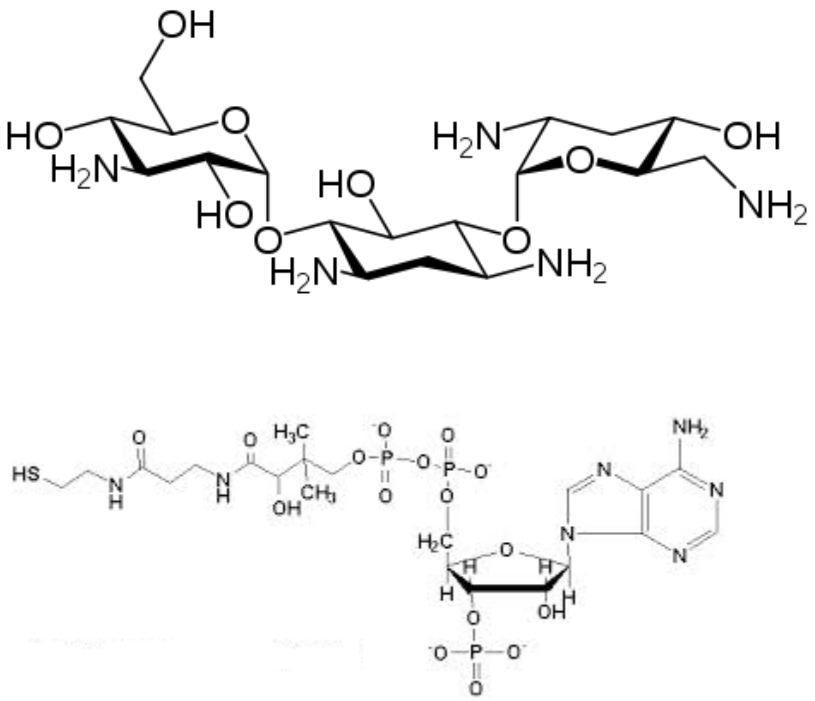

Figure 4: Structures of substrates used in this study (Top) aminoglycoside antibiotic Tobramycin and (Bottom) Co-substrate CoASH.

ii.The Aminoglycoside *N3* Acetyltransferase IIa:

The aminoglycoside *N3* acetyltransferase IIa (AAC-IIa) is a prokaryotic protein. It is 30.5-kDa constituting of 286 amino acids and is produced by gram-negative bacteria. AAC-IIa comprises about 85 percent of the clinical isolates that possess an AAC (3)-II type gene. AAC-IIa catalyzes the AcCoA-dependent acetylation of the amine group at the C3 position on an aminoglycoside antibiotic. AAC-IIa is a weakly promiscuous enzyme: it modifies the kanamycin class of aminoglycosides and has slow turnover rates when the neomycin class are substrates [36]. Thus far, this protein is the only AGME that has been characterized with least level of substrate promiscuity. No crystal structure is available for this enzyme, however a homology-derived model has been determined [36]. The large number of negatively charged side chains in the active site of the homology-derived model is consistent with other AGMEs, representing a large surface for the binding of positively charged aminoglycosides.

When comparing AAC-IIa, to AAC-IIIb and APH (3)-IIIa of similar molecular weight, AAC-IIa has about 70 percent sequence similarity with AAC-IIIb (Figure 3) and shares no homology (<5 percent) with APH (3')-IIIa. However, AAC-IIa, like APH (3')-IIIa, possess short amino acid segments considered to be disordered because they have been shown to be relatively flexible in an apo form by Nuclear Magnetic Resonance (NMR). NMR data acquired with this 30-kDa enzyme shows that, just like APH (3')-IIIa, the apo-enzyme is a highly dynamic protein displaying a significantly overlapped spectrum. In both cases, binding of aminoglycosides dramatically alter the NMR spectra, causing it to become well resolved, indicative of a well-defined structure of the protein in solution [21, 36, 37]. This does not seem to be the case for AAC-IIIb; it is structured in both its apo form and in binary complexes with its substrates. Yet, AAC-IIIb is

much more promiscuous than AAC-IIa [21, 36, 38, 39]. These observations suggest that enzymes that have high promiscuity are not necessarily more dynamic in structure than those with a lower promiscuity.

```
[AAC-IIa]       -------MHTQKAITEALQKLGVQSGDLLMVHASLKSIGPVEGGAETVVAALRSAVGPTG 53
[AAC-IIb]       MTSATASFATRTSLAADLAALGLAWGDAIMVHAAVSRVGRLLDGPDTIIAALRDTVGPGG 60
                       : *:.:::  *  **:  ** :****::. :* : .*.:*::****.:*** *

[AAC-IIa]       TVMGYASWDRSPYEETLNGA-RLDDNARRTWPPFDPATAGTYRGFGLLNQFLVQAPGARR 112
[AAC-IIb]       TVLAYADWEAR-YEDLVDDAGRVPPEWREHVPPFDPQRSRAIRDNGVLPEFLRTTPGTLR 119
                **:.**.*:   **: ::.* *:  : *.  *****  : : *. *:* :**  :**: *

[AAC-IIa]       SAHPDASMVAVGPLAETLTEPHELGHALGEGSPNERFVRLGGKALLLGAPLNSVTALHYA 172
[AAC-IIb]       SGNPGASLVALGAKAEWFTADHPLDYGYGEGSPLAKLVEAGGKVLMLGAPLDTLTLLHHA 179
                *.:*.**:**:*. ** :*  * *.:. *****  ::*. ***.*:*****:::* **:*

[AAC-IIa]       EAVADIPNKRWVTYEMPMPGRDGEVAWKTASDYDSNGILDCFAIEGKQDAVETIANAYVK 232
[AAC-IIb]       EHLADIPGKRIKRIEVPFATPTG-TQWRMIEEFDTG---DPIVAGLAEDYFAGIVTEFLA 235
                * :****.**    *:*:.   * . *:  .::*:.   * :.    :* .  *.. ::

[AAC-IIa]       LGRHREGVVGFAQCYLFDAQDIVTFGVTYLEKHFGTTPIVPAHEAIERSCEPSG 286
[AAC-IIb]       SGQGRQGLIGAAPSVLVDAAAITAFGVTWLEKRFGTPSP--------------- 274
                 *: *:*::* * . *.**  *.:****:***:***..
```

Figure 5: Sequence alignment of the two-acetyl transferases: AAC-IIa and AAC-IIIb. “*” Indicates conserved residues, “:” is an indication of conservation between groups of similar properties and “.” is an indication of the conservation between groups of weakly similar properties.

Since the AAC-IIa and AAC-IIIb are so similar in sequences it is likely that they are similar in structures as well. This leaves the question: what might be the reason for having such distinct substrate selectivity? This also suggests that, like AAC-IIIb, AAC-IIa also belongs to the GNAT superfamily of acetyl transferases. Superimposed structures of the AAC-IIa and AAC-IIIb show remarkable similarity to each other with a RMSD of 1.43Å. The region with the largest sequence differences between these two proteins is the loop region, amino acids 202-222 in AAC-IIa and 209-226 in AAC-IIIb [36].

Figure 6: Homology-derived, overlaid structures of AAC-IIa and AAC-IIIb. *Motif B*, the GNAT conserved acetyl acceptor site is shown in purple and the GNAT conserved region responsible for acetyl coenzyme A association is shown in yellow for both AAC-IIa and AAC-IIIb, the loops for AAC-IIa and AAC-IIIb are shown in green and blue respectively. Figure adapted with permission from Norris, A.L. and E.H. Serpersu, *Ligand promiscuity through the eyes of the aminoglycoside N3 acetyltransferase IIa.* Protein science: a publication of the Protein Society, 2013. 22(7): p. 916-28. Copyright © 2013 The Protein Society.

iii. Rationale of this study:

AAC-IIa has 35% amino acid sequence identity with AAC-IIIb, but in contrast to AAC-IIa, AAC-IIIb shows significantly less structural change associated upon binding of aminoglycosides. The region with the largest sequence differences between these two proteins is the loop region [21]. Previous NMR work shows that when AAC-IIa is in its apo form it has a very dynamic nature, seen by a number of overlapping peaks. When antibiotics such as tobramycin or kanamycin, bind the AAC-IIa, ^{15}N-^{1}H heteronuclear single quantum coherence (HSQC) spectra show significant increase in resolution and chemical shift range indicating a well- defined protein structure. This behavior is also observed in a high promiscuity enzyme APH (3')-IIIa shown in Figure 7 below.

Studies of the effect of solvent on AAC-IIIb-aminoglycoside interactions have revealed an interesting result that an opposite sign of change in heat capacity was observed when two structurally similar ligands were bound to the enzyme [39]. Another interesting property of AAC-IIIb was that several properties of the ternary enzyme-aminoglycoside-CoASH complex were dependent on the order of addition of substrates to the enzyme and these ternary complexes were not identical to each other. They displayed different hydrodynamic radii, NMR spectra and solvent protection [40].

In order to compare thermodynamic properties of both enzymes, we initiated studies with AAC-IIa. Denaturation curve on AAC-IIa, determined by differential scanning calorimetry (DSC) showed multiple transitions, which is novel amongst the AGMEs. The T_m of the first transition that was observed on the unfolding curve was at 29°C. Since all the previous data with AAC-IIa were collected at 25 °C examination of thermodynamics of AAC-

IIa at lower temperatures became necessary. Therefore, this work will focus on examining the unfolding transitions via biophysical techniques and the thermodynamic properties of enzyme–ligand complexes of AAC-IIa at temperatures below the first transition temperature observed in DSC.

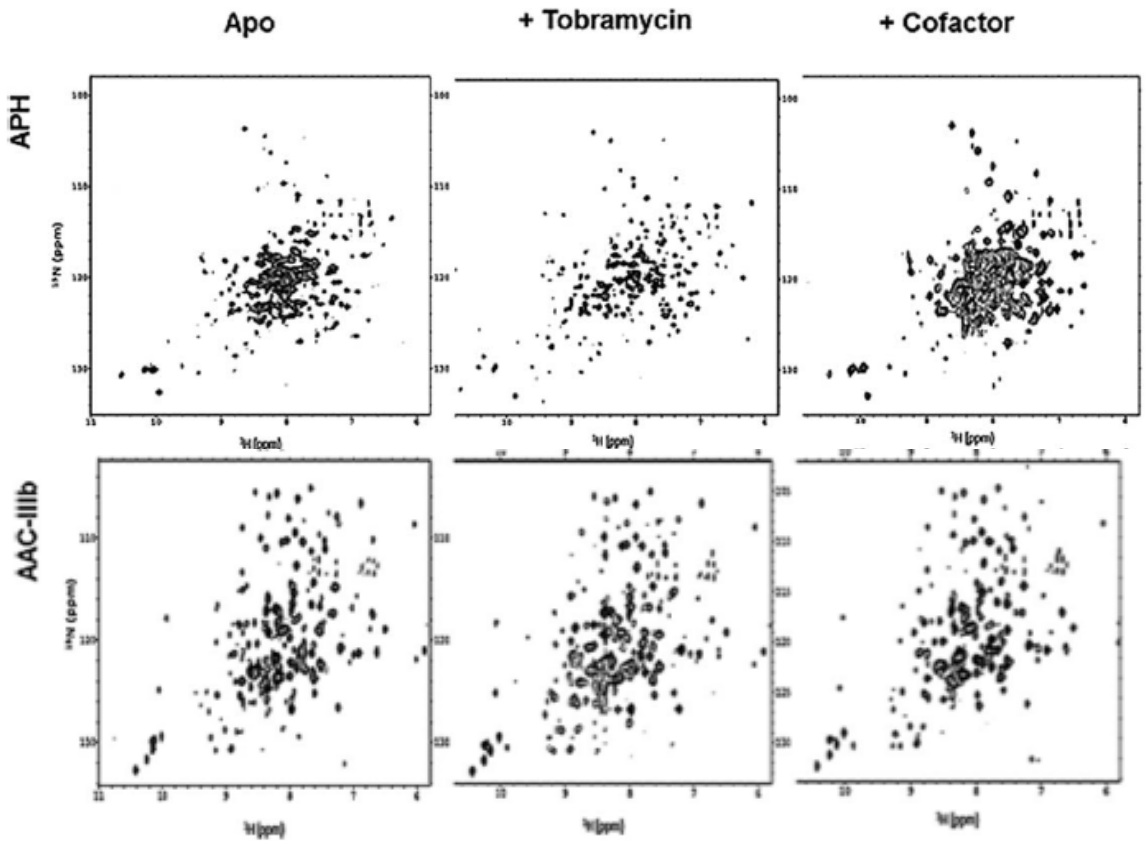

Figure 7: ^{1}H-^{15}N HSQC NMR spectra of AGMEs APH(3')-IIIa and AAC-IIIb and their complexes. Apo (left) , binary APH-tobramycin (middle) and binary APH-CoFactor (right) forms are shown. All spectra were taken under similar experimental conditions and shown to matching contour levels. Partial figure adapted with permission from Norris, A.L. and E.H. Serpersu, *Ligand promiscuity through the eyes of the aminoglycoside N3 acetyltransferase IIa.* Protein science: a publication of the Protein Society, 2013. 22(7): p. 916-28. Copyright © 2013 The Protein Society.

II. Methods

i. Materials:

Isopropyl- β-D-1-thiogalactopyranoside (IPTG) was purchased from Inalco Spa (Milano, Italy). Ion exchange matrix (Macro Q) was purchased from Bio-Rad Laboratories (Hercules, CA). High performance Ni-Sepharose resin was purchased from Amersham Biosciences (Piscataway, NJ). The purified thrombin was provided by Dr. Elias Fernandez (The University of Tennessee) or purchased from Enzyme Research Laboratories (South Bend, IN). 99.9% deuterium oxide and 99% ^{15}N enriched salts were purchased from Cambridge Isotope laboratories (Andover, MA). All the other reagents and AGs were purchased from Sigma -Aldrich (St. Louis, MO) at the highest possible purity.

ii. Overexpression and purification of AAC-IIa:

The AAC-IIa protein was overexpressed with IPTG using standard protocols in Luria Broth. The cells were harvested and stored at -80 °C and the enzyme was purified within two weeks from these cells. Purification of the AAC-IIa was performed using standard nickel affinity chromatography. Briefly, cells were suspended in 15 mL of lysis buffer (50mM Tris-HCl (pH 7.6), 100mM NaCl, 20 mM Imidazole, 200 μM PMSF at 4°C), lysed with a French press, and centrifuged for one hour at 34,000g. The supernatant was then passed through 1 mL of Ni-Sepharose resin where the AAC-IIa was eluted with a 100-350 mM imidazole gradient after extensive resin washing (50mM Tris-HCl (pH 7.6), 100mM NaCl, 20 mM Imidazole, at 4°C) to

>98% purity. The 6X- Histidine tag was removed by incubation with thrombin for 3hrs at 25 °C. Cleaved 6X-Histidine tag and un-cleaved protein were removed by passing through a Ni-Sepharose column. Histidine tag free protein was collected in flow-through. Following with a removal of thrombin by ion exchange chromatography where an increase of pH to 8.0 from 7.6 was required along with the removal of the NaCl by dialyzing it against 50mM Tris-HCl, pH 8.0 at 4°C. A strong anion exchange media MacroQ was used for this chromatography with an elution gradient of 0-750 mM NaCl. Lastly, the fractions containing AAC-IIa were dialyzed extensively against 50mM MOPS (pH 7.6) at 4°C and 100mM NaCl. The concentration of AAC-IIa was determined by using an $\varepsilon^{0.1\%}$ (280nm) of 1.16 spectrophometrically [36].

iii. Differential Scanning Calorimetry:

Differential Scanning Calorimetry (DSC) experiments were performed with AAC-IIa in buffer containing 50 mM MOPS and 100 mM NaCl on a VP-DSC micro calorimeter from MicroCal Inc. (Northampton, MA). The melting transition data was recorded from 2°C to 65°C for buffer with no protein, apo, binary and ternary complexes of the enzyme. For the binary and ternary complexes the protein concentration was maintained at 50 μM while the ligand concentrations were such that the enzyme was >98% saturated with the ligand. The unfolding curve for apo-AAC-IIa was measured at 30, 50 and 70 μM protein concentrations. The reference cell contained the final dialysate from protein preparation [50 mM MOPS buffer with 100mM NaCl] at pH 7.6. All samples were degassed for 20 minutes prior to injection. Origin software was used to analyze the data with a 2-state fitting model.

iv.Circular Dichroism:

Experiments were performed on an Aviv (Lakewood, NJ) model-202 spectrometer with a thermoelectric cell holder. 20-μM protein was placed in a cuvette with 2.0 mm path length. For the CD spectra as a function of temperature: The CD signal was measured at 222 nm with an increment of 0.2 °C temperatures. The sample was equilibrated for 0.2 minutes at a given temperature with a data averaging time of 5 seconds. For the CD spectra as a function of wavelength: The CD signal was measured over a wavelength range of 260 -190 nm with a wavelength step of 0.5nm at 25°C. The resulting spectrum was an average of four scans that had an averaging time of 1 second. Prior to all data collection the sample chamber was flushed with nitrogen gas.

v.Nuclear Magnetic Resonance:

AAC-IIa was uniformly ^{15}N-labelled using M9 minimal media containing ^{15}N NH_4Cl. Purification of the AAC-IIa was performed using the method described previously in this chapter under protein purification (section ii).

For NMR studies, the protein concentration was ~130 μM in 50mM MOPS and 100mM NaCl, pH 7.6. The tobramycin (ligand) was added to ensure >95% saturation as calculated from the dissociation constants [41]. All NMR experiments were performed using a 600-MHz, Varian Inova spectrometer equipped with a ^{1}H, ^{13}C, ^{15}N triple detection, salt tolerant cryogenic probe at the University of Tennessee. Sensitivity enhanced ^{1}H-^{15}N HSQC (heteronuclear single-

quantum coherence) correlation spectra [42] were recorded with a sweep width of 2434 Hz in proton dimension, 64 increments and 296 or more transients were acquired per slice.

Data were processed with NMRpipe Software [43]. FID was multiplied with a $\sin^2$ window function in the acquisition dimension before Fourier transformation. No baseline correction or other cosmetic procedures were applied. Spectra were exported to Sparky (T.D. Goddard and D.G. Kneller, SPARKY 3, University of California, San Francisco) for analysis and display. Enzymatic activities were determined before and after experiments and were >80% of the original activity.

vi. Analytical Ultra-Centrifugation:

The sedimentation velocity (SV) was performed in a Beckman XL-I analytical ultracentrifuge. Prior to centrifugation, the protein was dialyzed into 50mM MOPS (pH 7.6) and 100mM NaCl, and the resulting dialysate was used as the reference solution. After the addition of CoASH and/or aminoglycoside, 400 μL samples were placed in double-sector charcoal-filled epon cells. Samples were equilibrated for 2 hours under vacuum at 12°C and 25 °C and then run for 8 hours at 5000 rpm. Sedimentation of the enzyme was monitored by absorbance at 280nm. Sedimentation coefficients were determined by sedimentation coefficient distribution (*c(s)*) analysis using SEDFIT [44, 45] and the size distribution analysis of macromolecules was conducted using Lamm equation modeling [45].

vii. Isothermal Titration Calorimetry:

Isothermal Titration Calorimetry (ITC) Experiments were performed on a VP-ITC micro calorimeter purchased from Microcal, Inc. (Northampton, MA), at varying temperatures in a range of 4 – 29°C. AAC-IIa concentrations were between 20-30μM for the maintenance of *c* values ([Binding sites] x association constant) within the range of 1-100 for greater accuracy of association constant (K_A) measurements. The titrant solutions were prepared with desulphated aminoglycoside diluted into the final dialysis buffer used in the enzyme purification allowing both cell and syringe solutions to contain 100mM NaCl and 50mM of pH 7.6 MOPS at respective temperatures. Samples were degassed for 10 minutes before being loaded on to the instrument. The pH of each cell and syringe solution was checked before and after each experiment and no change was noticed. Titrations of substrate into enzyme solution consisted of 29 injections of 10μl, separated by 240 seconds with a cell stirring speed of 300rpm. The reference power was set to 10 μcal per second. The enzymatic activity of AAC-IIa was determined before and after each experiment. In all cases the enzyme activity remained greater than 85% of the starting activity.

Thermograms were integrated using the Origin software provided by the instrument manufacturer and the best fits were obtained using one-site binding. This data was also analyzed using the SEDPHAT [46]and NITPIC[47] softwares. The thermograms shown in figures are taken from the Origin software. Dissociation constants (K_D) values were calculated form the association constants (K_A) derived from fitted titration curves. The slope of plot of ΔH_{obs} versus temperature was used to determine the change in heat capacity (ΔCp).

viii. Kinetic Assays:

The kinetic parameters for the AAC-IIa activity were determined by using a continuous assay to determine enzyme activity, which utilizes the coupled reaction described below.

Tobramycin + Acetyl CoA → 3-Acetyl- Tobramycin +CoASH

4,4′ - Dipyridyl disulfide + CoASH → CoA –S-S-pyridine + pyridine -4-thiolate.

Activity of this enzyme is measured based on the reduction of 4,4′ - Dipyridyl disulfide by CoASH, releasing pyridine-4-thiolate, which can easily be detected at 324 nm spectrophometrically [48]. The concentration of AAC-IIa was determined by using a $\varepsilon^{0.1\%}$ (280nm) of 1.16 spectrophometrically. This was done using a Cary-Win UV-vis spectrophotometer (Varian, Palo Alto, CA). Samples comprised of 100mM NaCl and 50mM MOPS, pH 7.6 at varying temperatures. AAC-IIa (10*n*M) was used in each assay, and the reaction was initiated by addition of aminoglycoside tobramycin and substrate AcCoA concentration was held at the saturating level of 100 μM. Michaelis-Menten type kinetics were followed for the reaction with the substrate [26], where the substrate inhibition allowed data to fit the equation, $\nu = (V_{max}[S]) / (K_m + [S] + [S]^2/K_i)$, where ν is the initial velocity, V_{max} is the maximal velocity, K_m is the Michaelis constant, and K_i is the substrate inhibition constant. Turnover rates (k_{cat}) were calculated from the relationship $V_{max} = k_{cat}[E]_T$. All data were plotted and analyzed using GraphPad Prism version 6.00, GraphPad Software (San Diego, CA).

III. Results and Discussion

i. The unfolding of AAC-IIa shows multiple transitions

To initiate the comparative studies between the AAC-IIa and the AAC-IIIb, we started with the measurement of their melting temperatures (T_m). The melting temperature is the temperature at which each transition is 50 percent complete. For protein denaturation the T_m is the temperature at which 50 percent of the protein is unfolded and, assuming a two-state process, the remaining 50 is still in its native form or folded [49]. Thermal transitions of AAC-IIa in its apo, binary and ternary complexes were examined using differential scanning Calorimetry (DSC) over the temperature range of 2-65 °C. The DSC traces for AAC-IIa were not reversible; hence only T_m has been measured for qualitative conclusions. Table 1 below notes the melting temperatures of all the complexes of AAC-IIa.

DSC studies were performed with an enzyme concentration of 50 µM and a control run was performed with buffer solution as reference. Apo-AAC-IIa yielded a melting temperature of 43.9 °C. When a binary complex was formed with aminoglycoside tobramycin the melting temperature was determined to be 44.7°C. The binary enzyme–CoASH complex yielded a T_m value of 43.1°C. The melting temperature shift was 0.8°C higher with AAC-IIa –tobramycin complex and 0.8°C lower for AAC-IIa-CoASH complex as compared to apo-AAC-IIa. This shift is not significant, and hence it can be concluded that binding of ligands does not shift the T_m of AAC-IIa; i.e. the net unfolded protein in apo or ligand bound forms stays the same at that given temperature (Figure 8). Such was not the case in the AGME AAC-IIIb. Apo-AAC-IIIb, gave a T_m of 39.5°C while when bound to the aminoglycoside neomycin, the T_m drastically shifts to 44.8°C

[40]. This is another major difference between the two enzymes AAC-IIa and AAC-IIIb that share 70 percent sequence similarity with each other. AAC-IIa at the end of the run aggregates in both its apo and ligand bound form and thus the denaturation curve is not reversible and the data points after the aggregation point are not included in the representation below.

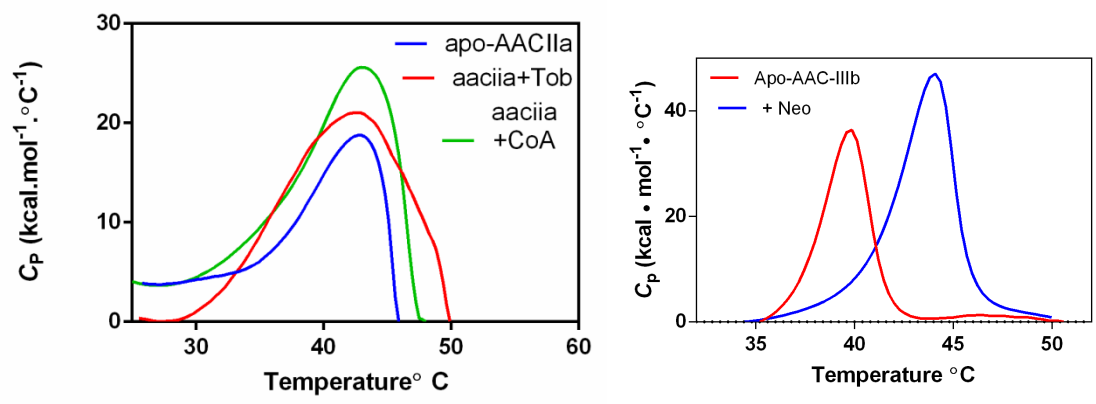

Figure 8: Denaturation curves of enzymes AAC-IIa (left) and AAC-IIIb (right) in their apo and binary complexes at temperature range 25-65 °C using DSC.

However, while examining melting of AAC-IIa, using DSC, a novel phenomenon was noticed amongst the AGMEs, two separate transitions were observed on the denaturation curve of AAC-IIa. The unfolding curve of apo-AAC-IIa showed two separate transitions with the melting temperatures of 29 °C and 43.9 °C respectively (Figure 9). Different concentrations of the enzyme were examined to check for a concentration-dependent behavior if any. Apo-AAC-IIa

was scanned at 30, 50 and 70 μM's respectively. All three concentrations led to the same melting temperatures showing a similar unfolding pattern (Figure 9-top panel).

To see the effect of addition of ligand to AAC-IIa, the thermal transitions of the binary complexes of AAC-IIa were examined (Figure 9, middle panel). Multiple transitions are observed below the T_m for both the binary complexes similar to the apo AAC-IIa. These observations state that the enzyme is undergoing various conformational changes at lower temperatures. At least one of the additional transitions at low temperature range, observed with both binary complexes, may represent dissociation of the ligand from the protein. This is a novel observation amongst the AGMEs. The sequence homolog AAC-IIIb does not show such additional transitions in apo or ligand-bound forms and also unlike AAC-IIa, upon binary complex formation the T_m shifts higher in a ligand-dependent manner.

The thermal transitions of the ternary complexes of AAC-IIa were also examined by using DSC. (Figure 9, bottom panel) Interestingly, upon formation of ternary complexes, regardless of the order of the complex formation, the melting temperature shifts drastically. For the addition of CoASH to the AAC-IIa-tobramycin complex, the melting temperature is 54.1°C and for the addition of tobramycin to the AAC-IIa-CoASH complex the melting temperature is 58.8°C. Similar to the unfolding pattern of apo and binary complexes of AAC-IIa, the ternary complexes also showed multiple transitions below T_m. Both ternary complexes show a significant upshift as compared to the apo and binary complexes of AAC-IIa. Hence, ternary complex formation is required to increase the melting temperature for AAC-IIa, which is unlike AAC-IIIb where a binary complex formation is sufficient to shift the melting temperature. These are also reminiscent of the differences between the ternary complexes of AAC-IIIb that are formed by

reversing the addition of ligands to the enzyme suggesting that such property may be more general than being specific for AAC-IIIb. NMR spectra of ternary complexes of AAC-IIa, show well dispersed spectra indicative of more structure and less flexibility at both 12°C and 29°C. However, it is seen that at 12°C, lower temperature, a ternary complex is a must for AAC-IIa to gain structure.

This observation of multiple transitions is indicative of various conformational changes that AAC-IIa undergoes at low temperatures. The final transition of apo AAC-IIa is higher than that of the AAC-IIIb, even though the AAC-IIa is more flexible. This suggests that the core structure of AAC-IIa is more heat resistant than AAC-IIIb.

Table 1: Melting temperatures acquired using differential scanning Calorimetry

Complex	Melting Temperature [°C]
Apo-AAC-IIa	43.9
AAC-IIa+Tobramycin	44.7
AAC-IIa-CoASH	43.1
[AAC-IIa+Tobramycin]+CoASH	54.1
[AAC-IIa+CoASH]+Tobramycin	58.8

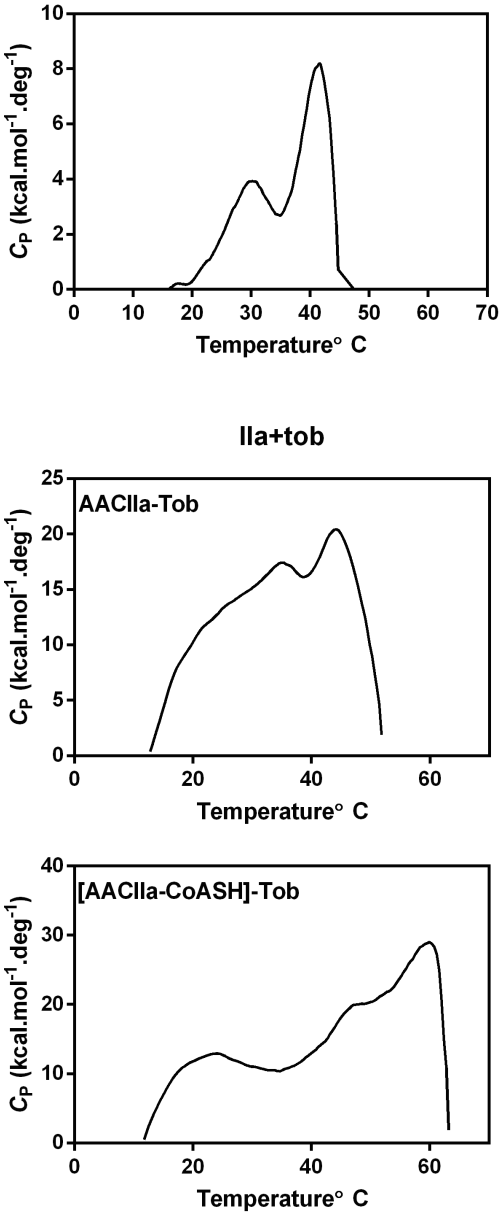

Figure 9: Unfolding curves showing multiple transitions of AAC-IIa in its apo (top panel) and binary (middle panel) and ternary (bottom) complexes.

ii.Melting temperatures of apo-AAC-IIa compared to its binary complexes are similar

To follow the α-helical melting, unfolding curves of AAC-IIa were observed using circular Dichroism (CD) spectroscopy. AAC-IIa does not yield a reversible signal as the protein aggregates, hence only the midpoint of unfolding transition (T_m) was determined in this study. Here, unfolding curves of AAC-IIa in its apo and binary complexes with tobramycin and CoASH were tested. Changes in α-helical content of the enzyme were followed at 222nm as a function of temperature. A sigmoidal curve pattern is observed for unfolding curves of all three complexes being tested (Figure 10). The melting temperature was determined from the mid points of these transition curves by using standard curve fitting procedure for a two-state process. Table 2 notes all the three melting temperature acquired from the CD analysis. One aspect of the data was consistent with DSC measurements, which are the midpoints of transitions did not show any effect of bound ligands and all yielded superimposable data.

T_m values determined by CD spectroscopy were ~10°C higher than those determined by DSC. CD spectra were collected as a function of wavelength to monitor the residual α-helical content. Spectra showing the α-helical content of apo AAC-IIa at selected temperatures are shown in figure 10 (bottom left panel). CD spectra acquired with the apo- and ligand-bound forms of the enzyme at temperatures corresponding to T_m determined by DSC revealed the presence of residual α-helical content for all complexes. The dip in figure 10 (bottom right panel) at 222 nm shows the presence of α-helical content at 45°C, a temperature above the T_m determined on DSC. The residual α-helical content at these temperatures might be protected due to aggregation and/or oligomerization. Required

temperature for the observation of spectra representing random coil was 60°C. These data are consistent with AAC-IIa being a highly flexible enzyme. It also suggest that unfolding of AAC-IIa occurs in multiple stages which may include unfolding of protein domains independent of each other and even at higher temperatures beyond $T_{m,}$ the enzyme still contains a structured core.

Table 2: Melting temperature measured via circular dichroism

Complex	T_m (°C)
Apo-AAC-IIa	54.5 ± 0.1
AAC-IIa-Tobramycin	53.6 ± 0.1
AAC-IIa-CoASH	52.6 ± 0.1

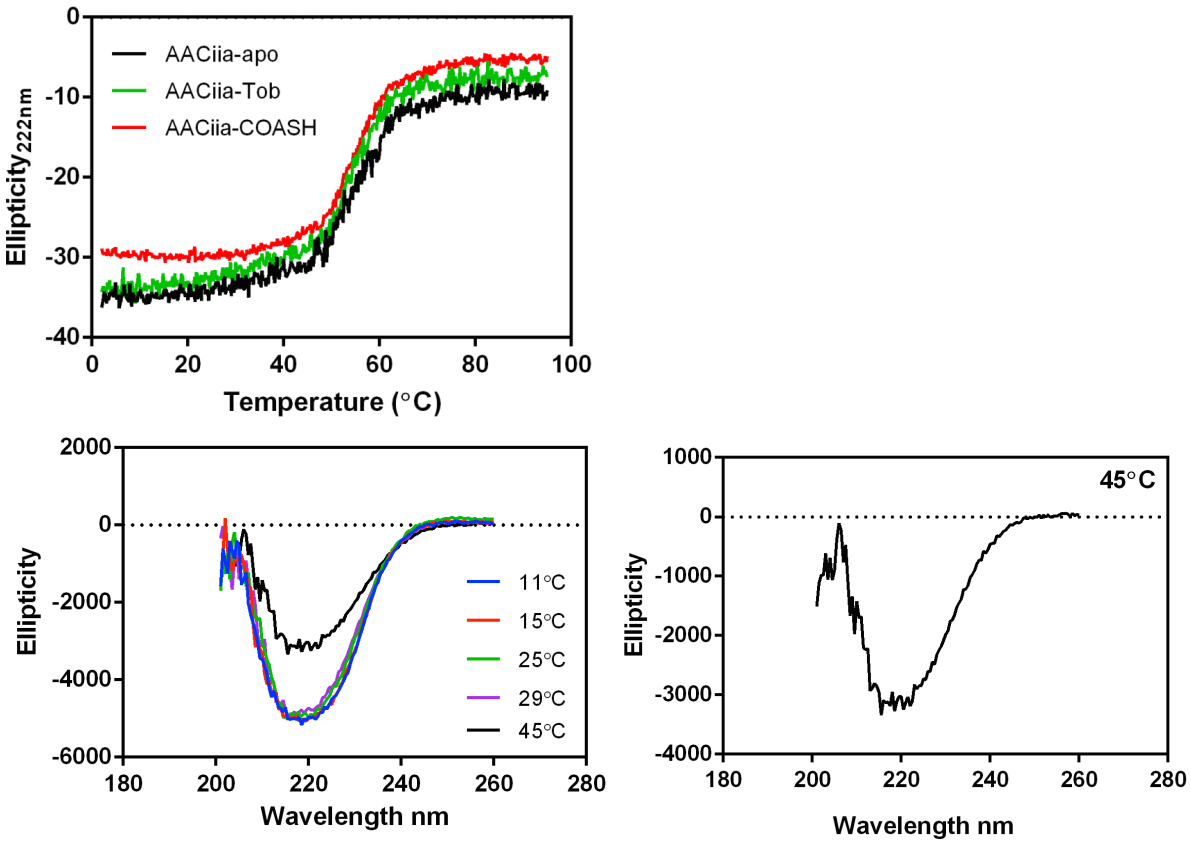

Figure 10: CD spectra of AAC-IIa: Unfolding of apo AAC-IIa and its binary complexes as a function of temperature acquired via CD (top panel); (bottom panel) (left) spectra showing the α-helical content of apo AAC-IIa at selected temperatures, (right) presence of α-helical content at 45°C.

iii.Thermodynamics of AAC-IIa at low temperatures

To determine thermodynamic properties of the formation of enzyme ligand complexes at temperatures below the first calorimetric transition peak, we titrated the enzyme with the tightest binding aminoglycoside tobramycin in studies with isothermal titration calorimetry (ITC). An example of ITC data is shown in figure 11 below. ITC data was collected over a

temperature range of 9-29°C and is noted in table 3 below. The binding affinity of tobramycin to the enzyme AAC-IIa decreases with increasing temperature. For instance, at 12°C, the tightest binding with a K_D of 12.2 ± 0.2 μM is observed, while the dissociation constant at 29 °C becomes 50.2 ± 1.1 μM. The binding enthalpies show more complex temperature dependence. For a temperature range of 9-20 °C, the ΔH_{obs} fluctuates within a small range of -5.6 and -8.6 kcal mol^{-1}, however for temperatures above 20 °C a bigger shift has been observed, suggesting that refolding or conformational changes of enzyme contributes to the observed enthalpy and contribution of refolding enthalpy steeply increased up to the melting temperature. These observations are consistent with NMR data where the binding of ligands cause the enzyme to adopt a well-defined structure at 29°C. No binding was observed for above 35°C presumably the active site is completely unfolded hence not capable of binding ligand.

Heat capacity is one of the major thermodynamic quantities that are measured in proteins and protein–ligand interactions. The change in heat capacity (ΔCp) is determined from the slope of the enthalpy versus temperature plots that are usually linear within a short temperature range. Since the binding enthalpy includes contributions at higher temperatures, we performed ligand binding at temperature well below the first transition temperature observed in DSC traces. For temperatures 9-20°C, where there is no contribution of enthalpy from conformational changes or refolding of the enzyme, the ΔH varies within a small range of -5.6 to -8.6 kcal mol^{-1} (Figure 12). ΔCp of -0.19 ± 0.1 kcal mol^{-1} K^{-1} was determined from the slope of the line from ΔH versus T for the temperature range below 20°C (Figure 13). This negative value of ΔCp suggests that the protein becomes "tighter" with increasing temperature and either more hydrophobic groups are buried or more hydrophilic groups are exposed to solvent

or both. Since the folding enthalpy of the protein starts to contribute to the measured enthalpy, the change in heat capacity above 20°C is not determined. Below 20°C, the binding enthalpy does not appear to have contribution of the folding enthalpy. The value of ΔCp below 20°C, is also similar to those determined for the carbohydrate-protein interactions, which are typically in the range of -0.1— -0.5 kcal mol^{-1} K^{-1}. Like AAC-IIa, the change in heat capacity for AAC-IIIb is also similar to values observed in carbohydrate-protein interactions [50]. Low temperature studies were required to discover this similarity of AAC-IIa and AAC-IIIb.

Table 3: Thermodynamic parameters of AAC-IIa binary complex with aminoglycoside Tobramycin.

Temperature (°C)	K_D (μM)	ΔH_{obs} (kcal mol^{-1})	$\Delta Cp_{(H20)}$ (kcal mol^{-1} K^{-1})
9	23.0 ± 0.6	-6.6 ± 0.6	
10	20.3 ± 0.6	-7.3 ± 0.6	-0.19 ± 0.1
12	12.2 ± 0.2	-6.2 ± 0.3	
13	23.2 ± 0.8	-5.6 ± 0.3	
15	14.5 ± 0.4	-7.7 ± 0.3	
17	24.2 ± 0.3	-7.1 ±0.5	
18	15.9 ± 0.4	-8.7 ± 0.4	
20	21.6 ± 0.3	-8.6 ± 0.7	
21	42.5 ± 2.2	-18.0 ± 1.8	
22	38.5 ± 0.2	-16.3 ± 2.1	
24	69.7 ± 2.1	-52.3 ± 2.3	
27	46.9 ± 1.2	-57.5 ± 2.6	
29	50.2 ± 1.1	-46.8 ± 3.0	

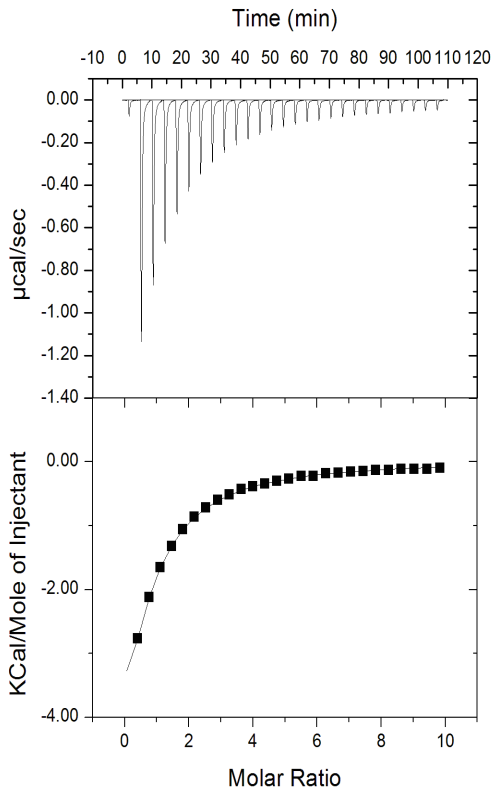

Figure 11: Typical thermogram (top) and isotherm (bottom) for titration of tobramycin into AAC-IIa. Time integration of the thermal power yields the heat of injection. In the isotherms, data points are shown with a fitted line to single-site binding.

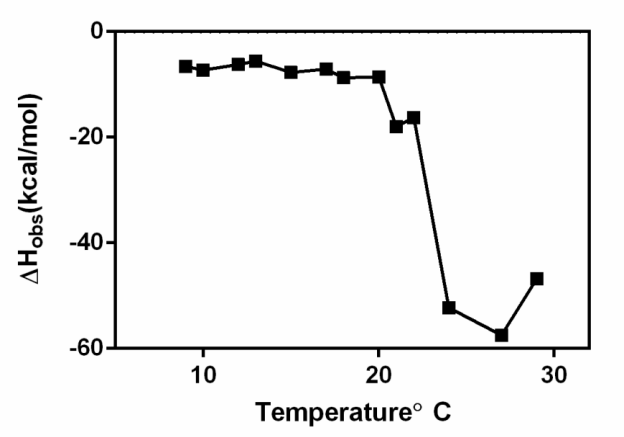

Figure 12: Changes in enthalpy of AAC-IIa with aminoglycoside tobramycin with increase in temperatures.

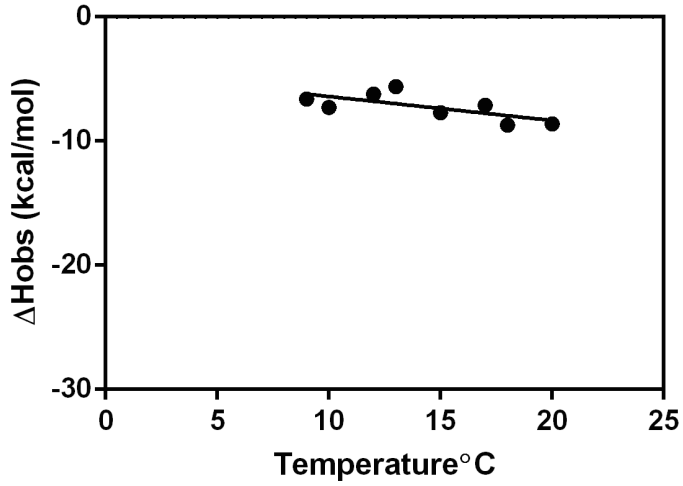

Figure 13: Determination of heat capacity change from the slope of the line obtained from plotting observed enthalpy against the increase in temperature

iv. Effect of temperature on the structure and complex formation of AAC-IIa.

The ITC data described in section iii show a tighter binding of aminoglycoside to AAC-IIa at lower temperatures. In light of these data we hypothesized that AAC-IIa may be more structured at temperatures below the first observed transition at 29°C. Hence, we studied AAC-IIa using nuclear magnetic resonance (NMR) at low temperatures. If this transition represents conversion of more structured regions of the protein to a more dynamic state, then the expectation is that the NMR spectra acquired below the transition temperature may reveal that AAC-IIa is indeed more structured at lower temperatures. NMR spectra were acquired and compared at 12°C well below the first transition observed in DSC and at 29°C, in its apo, binary and ternary complexes. Dynamic properties of a protein have profound effect on NMR spectra. This occurrence of a highly overlapped spectrum is a result of several backbone amide groups being in a very similar chemical environment indicative of protein being highly dynamic and adopting multiple conformations or has intrinsically disordered domains. However, the overall shifts and changes in the spectrum can still be examined.

Figure 14 is a representative of ^{1}H-^{15}N heteronuclear single quantum coherence (HSQC) spectra of apo AAC-IIa acquired at 12°C (spectra in red) and 29°C (spectra in green). Peaks are observed between a short chemical shift range of 7.21 to 8.40 ppm on the proton (^{1}H) x- axis and between 110.00 and 125.00 ppm on the (^{15}N) y-axis, yielding a highly overlapped spectrum. Examining the apo spectra at 29°C also shows a similar overlapped spectrum. Both spectra are indicative of highly dynamic protein at both temperatures. This observation strongly suggests that the transition at 29°C does not represent the conversion of a structured domain into a more flexible one. But may be indicative of a conformational change that may also include

contribution from the dissociation of ligand due to lowered affinity with increasing temperature.

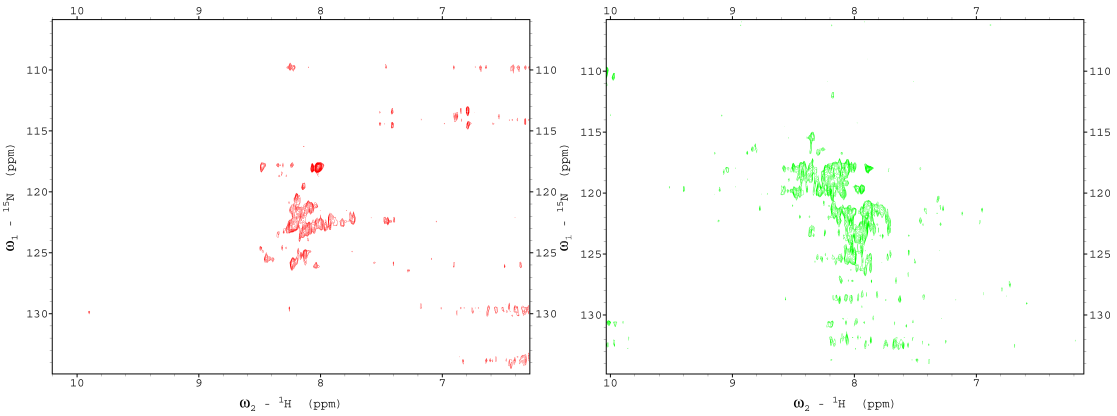

Figure 14: NMR spectra of ^{15}N labeled apo AAC-IIa: (left) spectra acquired at 12°C in red and (right) spectra acquired at 29°C in green.

To check how the structure of AAC-IIa changes upon the addition of ligand NMR spectra of binary complexes with aminoglycoside tobramycin and co-substrate CoASH are collected at both 12°C and 29°C. Spectra obtained from the binary complexes are shown in figure 15. Presence of ligands tobramycin (bottom panel) and CoASH (top panel) led to increase in the resolution of the spectrum acquired with the apo protein at 29°C and a relatively smaller changes in the spectrum collected at 12°C. The 12°C spectrum still maintained the highly overlapped character. Compared to CoASH, addition of tobramycin led to a little more dispersion of spectrum at 12°C giving a better resolution. This phenomenon is reversed when

the binary complexes were examined at 29°C. A better resolution is achieved upon binding of the co-substrate CoASH as compared to the aminoglycoside tobramycin. Binding of the ligands leads to some peak dispersion, however the spectra still remains overlapped. This suggests that AAC-IIa is still flexible and unstructured. These results are unlike AAC-IIIb. NMR spectra show AAC-IIIb is structured in its apo form. Addition of ligands show some dispersion but overall AAC-IIIb is structured [36].

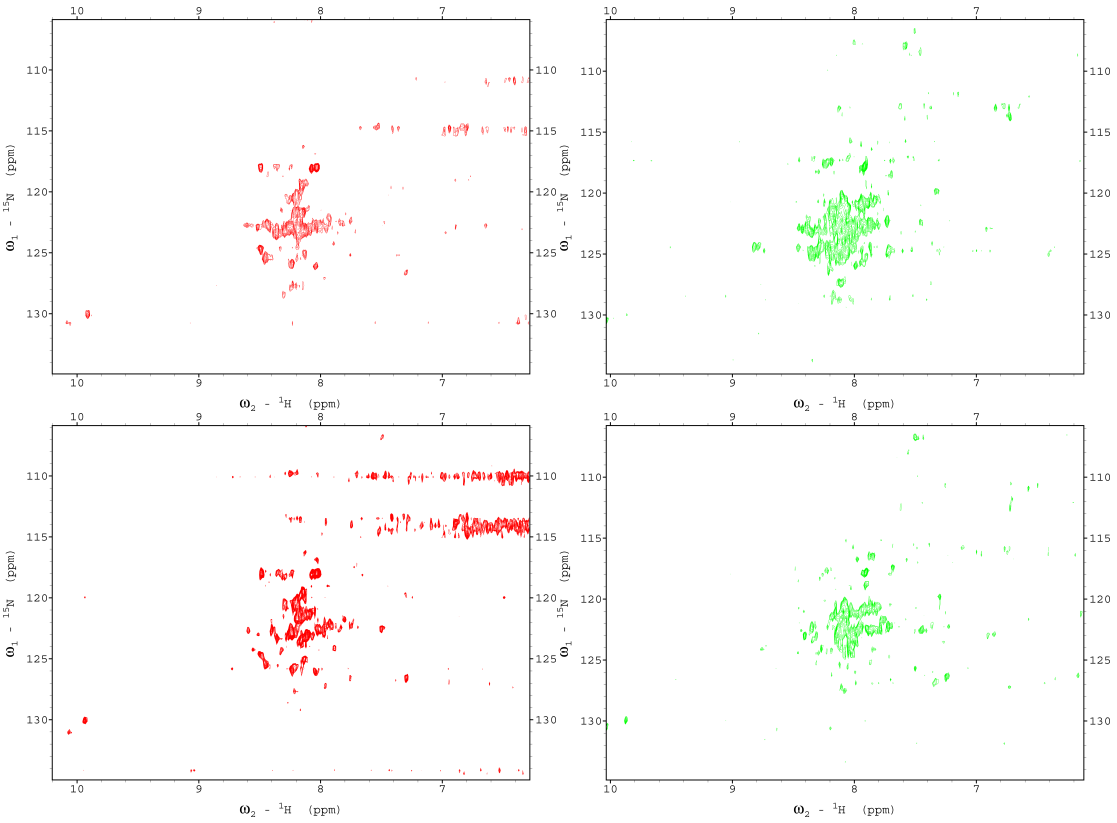

Figure 15: NMR spectra of binary complexes of ^{15}N labeled AAC-IIa at 12°C (red) and 29°C (green): (top) AAC-IIa-CoASH, (bottom) AAC-IIa- Tobramycin.

To observe the effect of formation of ternary complexes on the structure and dynamics of AAC-IIa, NMR spectra were acquired. Spectra were collected on the ternary complexes that were formed differently meaning to an AAC-IIa–co-substrate complex, tobramycin was added and to AAC-IIa-tobramycin complex CoASH were added (Figure 13). NMR spectrum of AAC-IIa, acquired at 12°C showed the highest dispersion in the ternary complexes indicating that both substrates are required for this enzyme to adopt a well-defined structure in solution. This is in contrast to its behavior at 29°C, where either CoASH or tobramycin alone can lead to a well-dispersed spectra. The spectra, acquired with ternary complexes, showed that there is slightly higher dispersion at both temperatures when CoASH binds to the enzyme first followed by tobramycin as compared to a ternary complex formed by addition of tobramycin first. Well-dispersed spectra are obtained in both the complexes at both the temperatures. This is an interesting property of AAC-IIa at 29°C addition of each ligand alone yields a well-dispersed spectra, however both ligand and the co-substrate are required to obtain good resolution at 12°C. This indicates that the conformations at 29°C are much more responsive to the addition of ligands, while the ones at 12°C are not. This is in contrast to AAC-IIIb, where it is structured in both its apo and ligand bound forms.

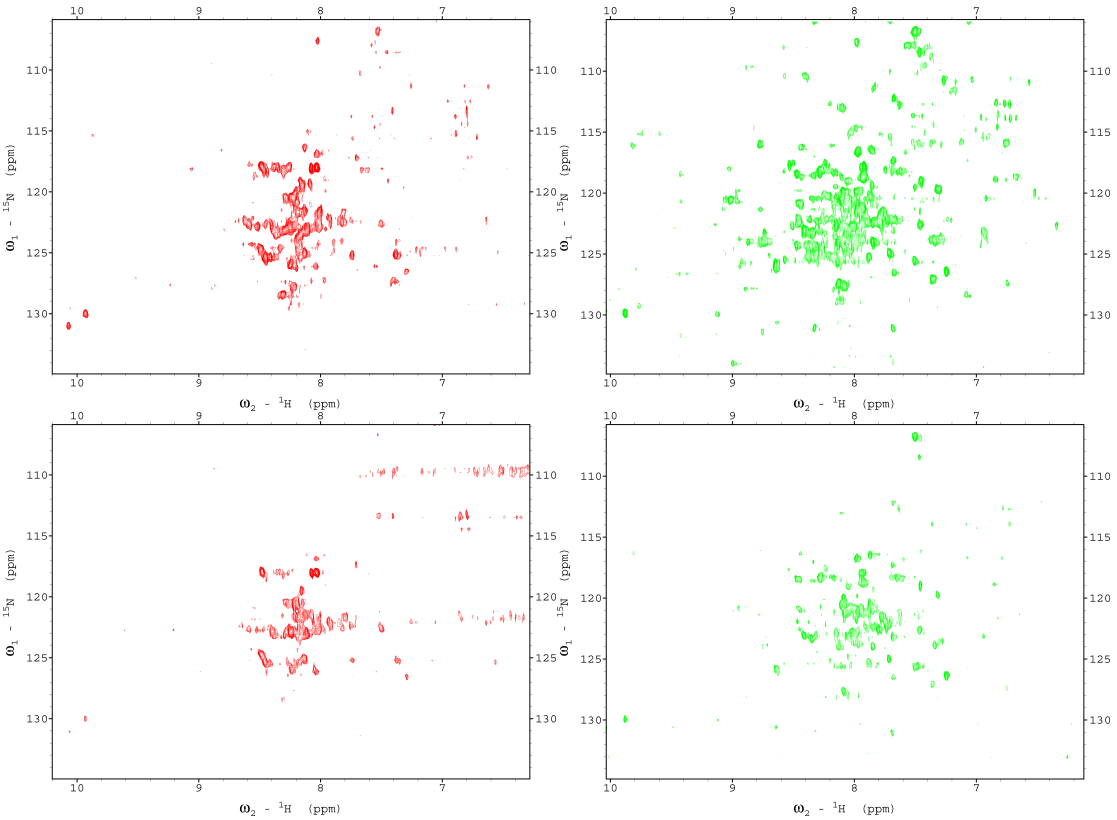

Figure 16: NMR spectra of ternary complexes of ^{15}N labeled AAC-IIa at 12°C (red) and 29°C (green): (top) [AAC-IIa-CoASH]-Tobramycin, (bottom) [AAC-IIa- Tobramycin]-CoASH.

When considering substrate promiscuity, this data becomes difficult to interpret. Rationally, enzymes with similar substrate profile should show similar NMR spectra and dynamic behavior; however such is not the case when it comes to these AGMEs. In the absence of ligand, a highly promiscuous enzyme, APH (3')-IIIa has a highly overlapped ^{1}H-^{1}5N-HSQC spectrum suggesting it is dynamic and flexible. Like AAC-IIa, upon binding of aminoglycoside tobramycin it gains a well-defined structure and unlike AAC-IIa the binding of co-substrate Mg-ATP causes minimal change to the spectra as compared to its apo form [36]. The presence of co-substrate alters the conformation of AAC-IIa, as the spectrum becomes more dispersed in

both binary and ternary complexes at both temperatures. AAC-IIa shows dynamic behavior like the APH (3')-IIIa, while AAC-IIIb doesn't but substrate profiles of AAC-IIIb and APH (3')-IIIa are highly similar and significantly different than that of AAC-IIa. Thus, these results indicate that flexibility alone cannot account for the substrate promiscuity.

v. Structural characterization of AAC-IIa

To determine whether the conformational changes and the structural changes observed via NMR spectra were not due to formation of dimeric or oligomeric species of the enzyme, AAC-IIa was studied using Analytical ultracentrifugation (AUC). AUC data was collected at both 12°C and 25 °C.

The structure of AAC-IIa was tested in its apo form with varying concentrations as well as in its binary and ternary complex states by AUC. Initial experiments at 25 °C with 50 μM AAC-IIa in the absence of substrate at 25 °C showed a sharp peak (Figure 14) with a sedimentation coefficient (*S*) of 2.7 and a frictional ratio (f/f_o) of 1.33. These values indicate a molecular weight of 30.9-kDa. The molecular weight of AAC-IIa is 30.5-kDa, so this data suggest that AAC-IIa is in a monomeric state in its apo form at 50 μM protein concentration. To test the concentration dependence of monomer-dimer equilibrium, if any, two additional concentrations, 30 μM and 70 μM, were tested for the apo AAC-IIa at 25 °C (Figure 17). The enzyme was monomeric at both concentrations with *S*- values of 2.7 and molecular weight of 30.9-kDa Binary complexes of AAC-IIa with aminoglycosides at saturating levels of tobramycin and co-substrate, CoASH, at 50 μM enzyme concentration, were tested at 25 °C (Figure 18). There was no shift in the *S*- values

in the data collected with the binary complexes and neither a shift in the frictional ratio nor a change in the molecular weight was observed. Data acquired with two ternary complexes that were formed with reverse addition of tobramycin and CoASH to the enzyme was also examined (Figure 19). Like binary complexes, ternary complexes also showed results similar to apo-AAC-IIa at 25 °C. These observations show that AAC-IIa remains monomer with bound ligands at 25 °C.

Interesting results were seen from studies of AAC-IIa at 12 °C. The apo AAC-IIa at 12 °C, is found to be dimeric with an f/f_o of 1.2 and molecular weight of 59.8-kDa. However, ligand binding to form either binary or ternary complexes drives AAC-IIa to become a monomer. For the binary and ternary complexes the f/f_o was found to be 1.2 and a sedimentation coefficient 2.3 giving a molecular weight of 30.4-kDa. AUC studies have shown that, AAC-IIIb exists as a dimer in its apo state as well as in various binary and ternary complexes [40]. Conversely, AAC-VIa, another acetyl transferase with the most limited substrate profile, forms a dimer with increasing concentrations in its apo form, while with binding of aminoglycosides or co-substrate CoASH, in either its binary or ternary complexes drives the enzyme to become a monomer [Kumar and Serpersu, unpublished]. Literature also shows that unlike AAC (6')-Ii and AAC (6')-Iy that exist as dimers, AAC (6')-Ib and AAC (6')-Ib-cr are monomers and AAC (6')-Ib11 exhibits a monomer-dimer equilibrium [51].

Apo AAC-IIa at 12 °C is a dimer and at 25 °C is a monomer, which support the multiple transitions observed in the unfolding of AAC-IIa such that the first transition may include conversion of dimer to monomer. These observations highlight a difference between the AAC-IIIb and AAC-IIa despite a ~70 percent sequence similarity between them. It also appears from

these observations that perhaps dimerization could be the cause for a more structured enzyme.

This may cause more structural control on the active site to increase ligand promiscuity.

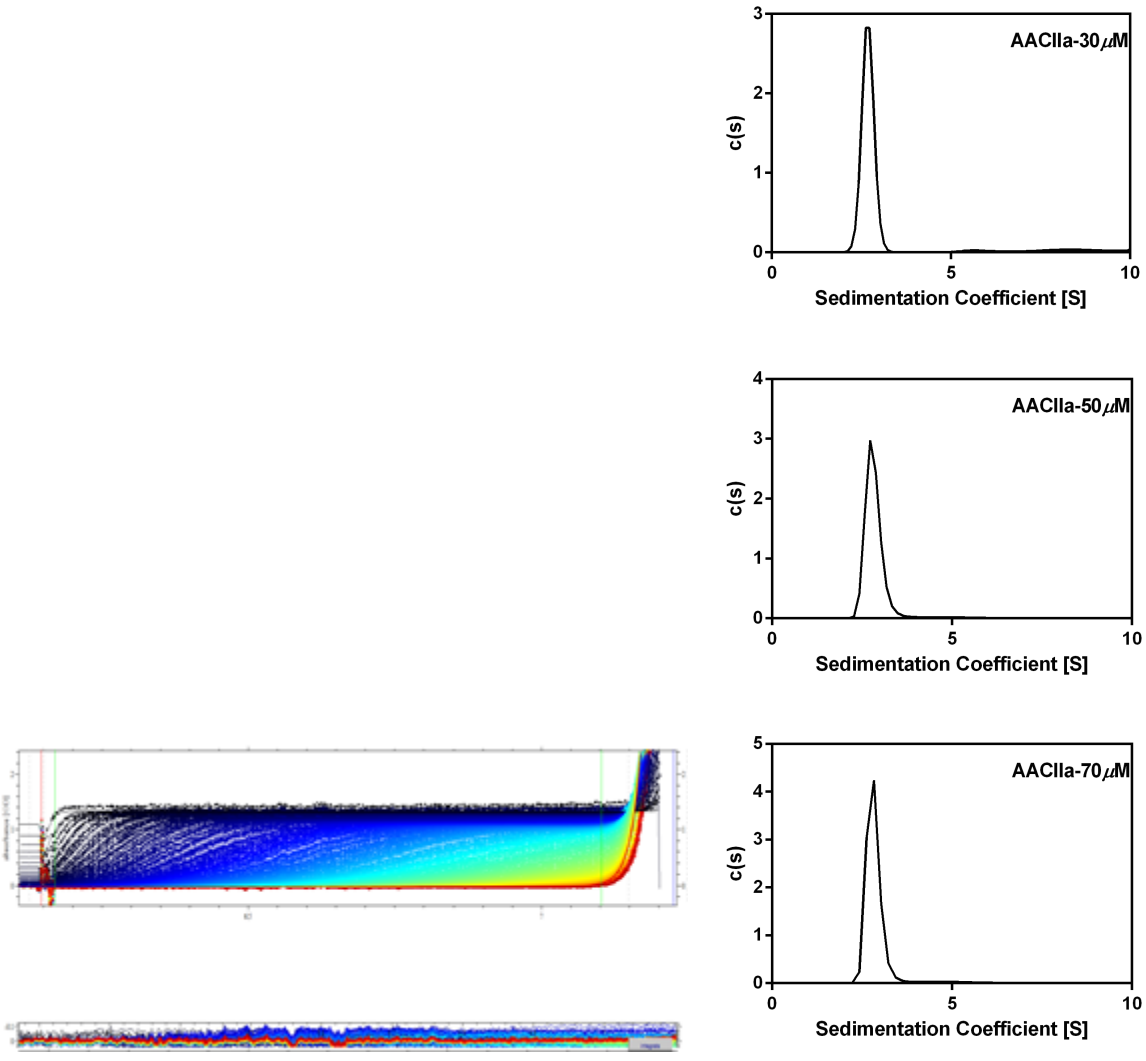

Figure 17: AUC studies of apo-AAC-IIa at varying concentrations shows it's a monomer
Analytical ultracentrifugation representative raw data acquired by analytical ultracentrifugation are shown in the left panel with sedimentation plots for all complexes shown in the right panel.

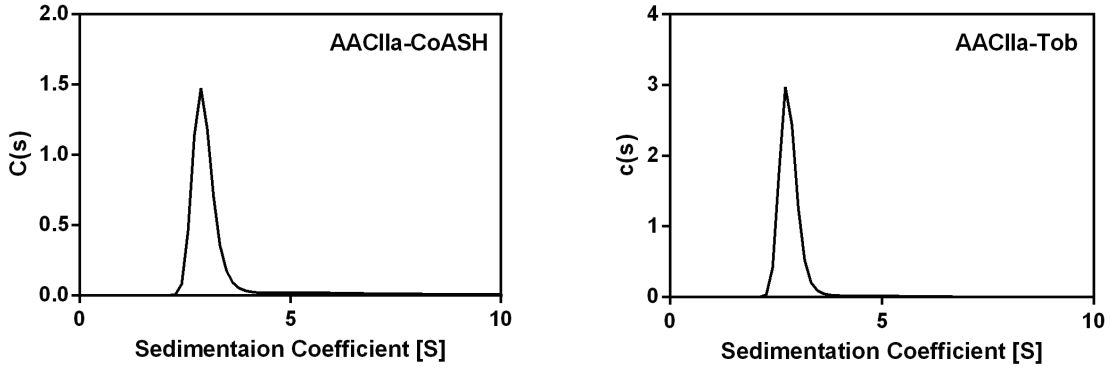

Figure 18: Sedimentation plot obtained from AUC studies of binary complexes of AAC-IIa with aminoglycoside: tobramycin and co-substrate CoASH.

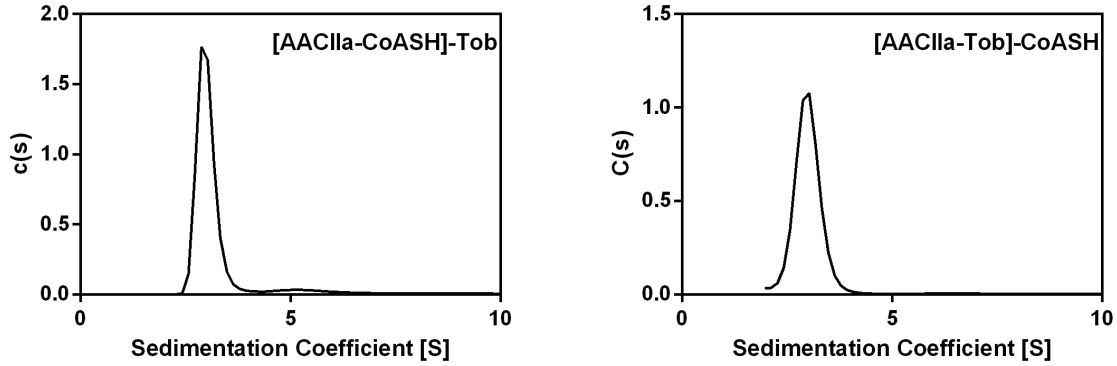

Figure 19: Sedimentation plot obtained from AUC studies of ternary complexes of AAC-IIa formed two ways.

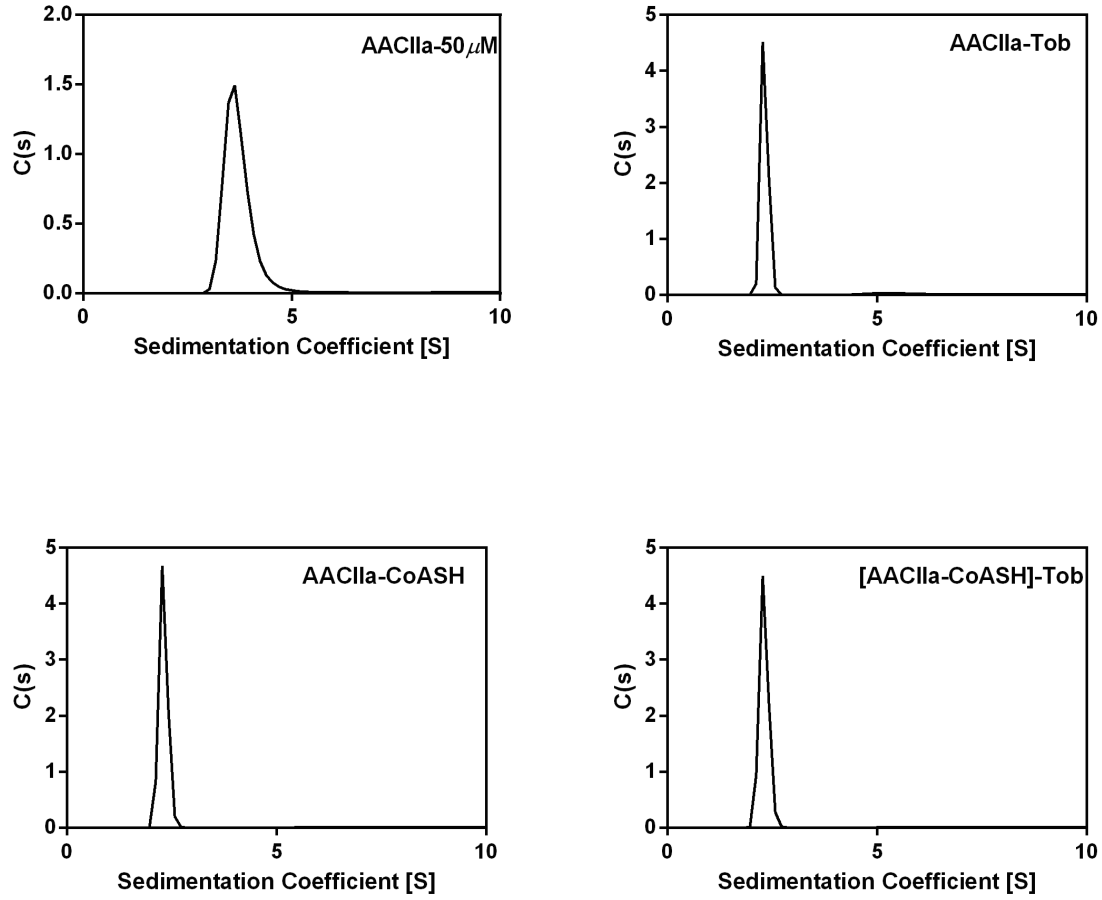

Figure 20: Sedimentation plot obtained from AUC studies of complexes of AAC-IIa at 12°C

vi.Examining catalysis of AAC-IIa at low temperatures

Unfolding of AAC-IIa showed the presence of various transitions indicative of conformational changes at low temperatures. However, NMR spectra revealed that, at lower temperatures the protein is still highly dynamic and has disordered regions. The catalytic activity of AAC-IIa is observed over a temperature range of 10 – 29°C to see if the conformational changes have any effect of the activity.

The aminoglycoside tobramycin was used to examine the temperature dependence of catalysis of AAC-IIa. The rates increased steadily between temperatures 10 °C and 27°C and started dropping from temperatures 29°C and above (Figure 20). There is a steady increase in activity at the early parts of the transitions and at 29°C AAC-IIa starts loosing activity. 29°C is the midpoint of the first transition observed in DSC. This suggests that the first transition observed in DSC studies may represent melting of the active site as reflected in loss of activity above this temperature.

These data obtained from the temperature dependence study (Table 4) were used to make a van't Hoff plot, which is a graph of natural log of k_{cat} as a function of inverse temperature (Figure 21). The slope of this line gives the activation enthalpy. The slope being negative states that the reaction is endothermic and the activation energy was calculated to be 12.6 ± 0.5 kcal/mol. The activation energy is the minimum amount of energy required by the enzyme to overcome the energy barrier for the reaction to proceed [52]. The activation energy was found to be 11.6 kcal/mol for AAC-IIIb with kanamycin A as substrate [Norris and Serpersu, unpublished]. Since activation energies for AAC-IIa and AAC-IIIb are similar, it is likely that the reaction mechanism is identical for both enzymes. Another AGME,

aminoglycoside nucleotidyltransferase (2")-Ia (ANT (2")-Ia) that catalyzed nucleotidylation of aminoglycosides has significantly higher activation energy (19.2 kcal/mol) than the acetylation reactions catalyzed by these two enzymes. [53]

Table 4: Kinetic parameters of AAC-IIa

Temperature (°C)	1000/T (°K)	Specific activity (μmol/min/mg)	k_{cat} (s-1)	ln k_{cat}
10	3.53	10.5 ± 0.4	5.7	1.8
12	3.51	11.6 ± 0.6	6.4	1.9
15	3.47	16.1 ± 0.6	8.8	2.2
17	3.45	21.5 ± 1.1	11.8	2.5
19	3.42	24.1 ± 1.8	13.2	2.6
21	3.40	26.7 ± 0.3	14.6	2.7
23	3.30	32.0 ± 1.5	17.5	2.9
25	3.35	32.9 ± 3.3	18.0	2.9
27	3.33	42.0 ± 1.8	23.0	3.1
29	3.31	38.5 ± 1.5	21.1	3.1

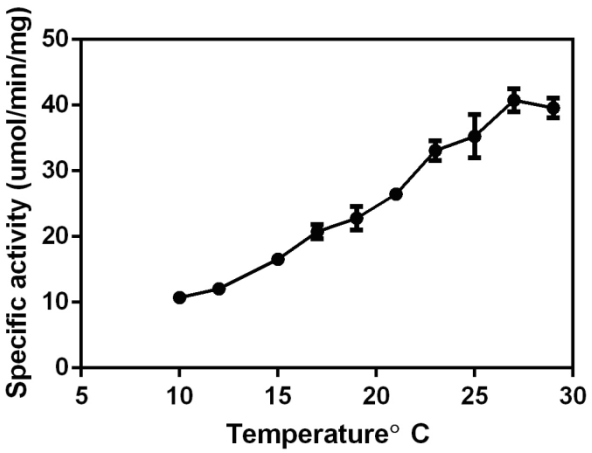

Figure 21: Plot of Specific activity of AAC-IIa with Tobramycin as a function of temperature.

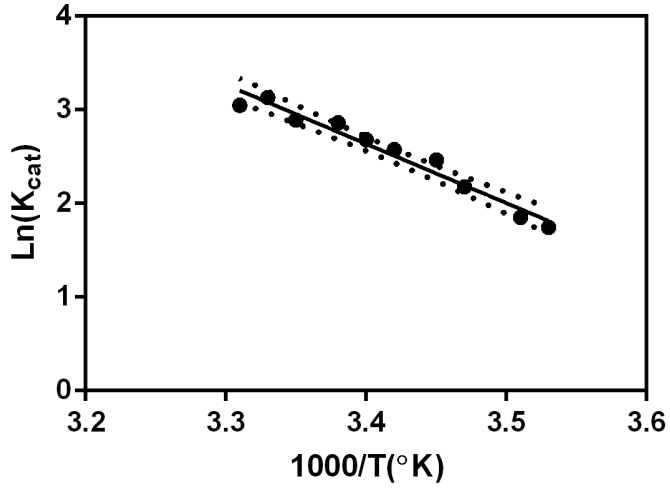

Figure 22: Temperature dependence of catalysis by AAC-IIa using tobramycin as substrate

Chapter 3: Conclusion and Future Directions:

This work demonstrates that AAC-IIa undergoes conformational changes at low temperatures, which represents a novel property amongst the AGMEs. Noticeably, this behavior is unlike that characterized for AAC-IIIb. The overlapped NMR spectra and multiple transitions observed in DSC studies suggest that the enzyme AAC-IIa, unlike AAC-IIIb, is flexible and dynamic. Both AAC-IIa and AAC-IIIb have heat capacity change consistent with carbohydrate protein interactions, in agreement with their proposed mode of action. Like most of the AACs, AAC-IIa originates from a soil bacterium. At 12°C, which is below the average soil temperature of ~25°C, AAC-IIa is a dimer in its apo form and it becomes monomeric upon formation of a complex with its substrate. However, it is a monomer regardless of substrate binding at 25°C while AAC-IIIb is always a dimer, irrespective of temperature. These results suggest that the enzymes might have coevolved in order to over come the changes in temperature.

When considering substrate promiscuity, these data become difficult to interpret. Rationally, more dynamic behavior the enzyme portrays, the more promiscuous it is. However, experimental evidence obtained here indicates that it is not the case for these classes of AGMEs. From the properties highlighted in this work, dimerization may be a key difference in explaining the distinct substrate profiles between AAC-IIa and AAC-IIIb. Dimerization provides these enzymes with more structure. Structural stability, in-turn, decreases the enzymes' dynamics and thereby stabilizing the active site conformation in order to accept various

antibiotics including neomycins. It is also possible that AAC-IIIb has evolved to become a dimer, allowing flexibility of active sites aiding in promiscuity. It has been shown in a computational work combined with NMR data, by Norris et.al, that the binding of CoASH to AAC-IIIb increases the flexibility of the loop region of the antibiotic binding site and renders the motion of the loop residues cooperative. Another reason for the differences in substrate profiles could be the difference in mobility of the loop region of the antibiotic binding site that is common in both enzymes, but future work will be necessary to explore this possibility.

The work presented here provides insights in the properties of AAC-IIa but more information is required to fully understand these systems and the implications on ligand promiscuity. Future studies could include, but are not limited to, the role of solvent in protein-ligand interactions, amino-acid specific labeling of AAC-IIa for NMR spectral assignments, X-ray crystal structures in its unbound and various ligand bound forms, NMR detected relaxation dispersion to quantify and characterize different conformations that AAC-IIa undergoes.

References:

1. UMEZAWA, H., *Biochemical Mechanism of Resistance to Aminoglycoside Antibiotics*, in *Advances in Carbohydrate Chemistry and Biochemistry*, T.a. HORTON, Editor. 1974, Harcourt Brace Jovanovich p. 184-225.
2. Voss, J.G., *Lysozyme Lysis of Gram-Negative Bacteria without Production of Spheroplasts.* Journal of general microbiology, 1964. **35**: p. 313-7.
3. DAVIES, J.E., *Aminoglycoside-Aminocyclitol Antibiotics and Their Modifying Enzymes*, in *Antibiotics in Laboratory medicine*, V.Lorean, Editor. 1991, Williams and Williams: Baltimore, MD. p. 691-713.
4. Drew, R.H., *Aminoglycosides.* Uptodate, 2014.
5. Ennifar, E., et al., *Targeting the dimerization initiation site of HIV-1 RNA with aminoglycosides: from crystal to cell.* Nucleic Acids Res, 2006. **34**(8): p. 2328-39.
6. Clardy, J., M.A. Fischbach, and C.R. Currie, *The natural history of antibiotics.* Curr Biol, 2009. **19**(11): p. R437-41.
7. Dewick, P.M., *Medicinal Natural Products: A Biosynthetic Approach.* Wiley, 2009. **ISBN 0-470-74167**(3rd edition).
8. Lynch, S.R. and J.D. Puglisi, *Structural origins of aminoglycoside specificity for prokaryotic ribosomes.* J Mol Biol, 2001. **306**(5): p. 1037-58.
9. Hammes, W.P. and F.C. Neuhaus, *On the mechanism of action of vancomycin: inhibition of peptidoglycan synthesis in Gaffkya homari.* Antimicrob Agents Chemother, 1974. **6**(6): p. 722-8.
10. Tenson, T., M. Lovmar, and M. Ehrenberg, *The mechanism of action of macrolides, lincosamides and streptogramin B reveals the nascent peptide exit path in the ribosome.* J Mol Biol, 2003. **330**(5): p. 1005-14.
11. Vicens, Q. and E. Westhof, *Crystal structure of paromomycin docked into the eubacterial ribosomal decoding A site.* Structure, 2001. **9**(8): p. 647-58.
12. Rinehart, K.L., Jr. and R.M. Stroshane, *Biosynthesis of aminocyclitol antibiotics.* J Antibiot (Tokyo), 1976. **29**(4): p. 319-53.
13. Liu, M., et al., *Tethered bisubstrate derivatives as probes for mechanism and as inhibitors of aminoglycoside 3'-phosphotransferases.* J Org Chem, 2000. **65**(22): p. 7422-31.
14. Fourmy, D., et al., *Structure of the A site of Escherichia coli 16S ribosomal RNA complexed with an aminoglycoside antibiotic.* Science, 1996. **274**(5291): p. 1367-71.
15. Recht, M.I., et al., *RNA sequence determinants for aminoglycoside binding to an A-site rRNA model oligonucleotide.* J Mol Biol, 1996. **262**(4): p. 421-36.
16. Kotra, L.P., J. Haddad, and S. Mobashery, *Aminoglycosides: perspectives on mechanisms of action and resistance and strategies to counter resistance.* Antimicrob Agents Chemother, 2000. **44**(12): p. 3249-56.
17. Pfister, P., et al., *The molecular basis for A-site mutations conferring aminoglycoside resistance: relationship between ribosomal susceptibility and X-ray crystal structures.* Chembiochem, 2003. **4**(10): p. 1078-88.
18. Vicens, Q. and E. Westhof, *Molecular recognition of aminoglycoside antibiotics by ribosomal RNA and resistance enzymes: an analysis of x-ray crystal structures.* Biopolymers, 2003. **70**(1): p. 42-57.

19. Vicens, Q. and E. Westhof, *Crystal structure of geneticin bound to a bacterial 16S ribosomal RNA A site oligonucleotide.* J Mol Biol, 2003. **326**(4): p. 1175-88.
20. Serpersu, E.H., et al., *Conformations of antibiotics in active sites of aminoglycoside-detoxifying enzymes.* Cell Biochem Biophys, 2000. **33**(3): p. 309-21.
21. Serpersu, E.H. and A.L. Norris, *Effect of protein dynamics and solvent in ligand recognition by promiscuous aminoglycoside-modifying enzymes.* Advances in carbohydrate chemistry and biochemistry, 2012. **67**: p. 221-48.
22. Ozen, C., J.M. Malek, and E.H. Serpersu, *Dissection of aminoglycoside-enzyme interactions: a calorimetric and NMR study of neomycin B binding to the aminoglycoside phosphotransferase(3')-IIIa.* Journal of the American Chemical Society, 2006. **128**(47): p. 15248-54.
23. Serpersu, E.H. and A.L. Norris, *Effect of Protein Dynamics and Solvent in Ligand Recognition by Promiscuous Aminoglycoside-Modifying Enzymes.* Advances in Carbohydrate Chemistry and Biochemistry, 2012. **in press**.
24. Shaw, K.J., et al., *Molecular genetics of aminoglycoside resistance genes and familial relationships of the aminoglycoside-modifying enzymes.* Microbiol Rev, 1993. **57**(1): p. 138-63.
25. Shaw, K.J., et al., *Molecular genetics of aminoglycoside resistance genes and familial relationships of the aminoglycoside-modifying enzymes.* Microbiological reviews, 1993. **57**(1): p. 138-63.
26. McKay, G.A. and G.D. Wright, *Kinetic mechanism of aminoglycoside phosphotransferase type IIIa. Evidence for a Theorell-Chance mechanism.* J Biol Chem, 1995. **270**(42): p. 24686-92.
27. Toth, M., et al., *Crystal structure and kinetic mechanism of aminoglycoside phosphotransferase-2''-IVa.* Protein Sci, 2010. **19**(8): p. 1565-76.
28. Hon, W.C., et al., *Structure of an enzyme required for aminoglycoside antibiotic resistance reveals homology to eukaryotic protein kinases.* Cell, 1997. **89**(6): p. 887-95.
29. Wybenga-Groot, L.E., et al., *Crystal structure of an aminoglycoside 6'-N-acetyltransferase: defining the GCN5-related N-acetyltransferase superfamily fold.* Structure, 1999. **7**(5): p. 497-507.
30. Toth, M., S. Vakulenko, and C.A. Smith, *Purification, crystallization and preliminary X-ray analysis of Enterococcus casseliflavus aminoglycoside-2''-phosphotransferase-IVa.* Acta Crystallogr Sect F Struct Biol Cryst Commun, 2010. **66**(Pt 1): p. 81-4.
31. Shi, K., D.R. Houston, and A.M. Berghuis, *Crystal structures of antibiotic-bound complexes of aminoglycoside 2''-phosphotransferase IVa highlight the diversity in substrate binding modes among aminoglycoside kinases.* Biochemistry, 2011. **50**(28): p. 6237-44.
32. Vetting, M.W., et al., *Structure and functions of the GNAT superfamily of acetyltransferases.* Arch Biochem Biophys, 2005. **433**(1): p. 212-26.
33. Azucena, E. and S. Mobashery, *Aminoglycoside-modifying enzymes: mechanisms of catalytic processes and inhibition.* Drug Resist Updat, 2001. **4**(2): p. 106-17.
34. Houghton, J.L., et al., *The future of aminoglycosides: the end or renaissance?* Chembiochem, 2010. **11**(7): p. 880-902.

35. Carew, J.S., et al., *Targeting autophagy augments the anticancer activity of the histone deacetylase inhibitor SAHA to overcome Bcr-Abl-mediated drug resistance.* Blood, 2007. **110**(1): p. 313-22.
36. Norris, A.L. and E.H. Serpersu, *Ligand promiscuity through the eyes of the aminoglycoside N3 acetyltransferase IIa.* Protein science : a publication of the Protein Society, 2013. **22**(7): p. 916-28.
37. Norris, A.L. and E.H. Serpersu, *NMR detected hydrogen-deuterium exchange reveals differential dynamics of antibiotic- and nucleotide-bound aminoglycoside phosphotransferase 3'-IIIa.* Journal of the American Chemical Society, 2009. **131**(24): p. 8587-94.
38. Hu, X., et al., *Coenzyme A binding to the aminoglycoside acetyltransferase (3)-IIIb increases conformational sampling of antibiotic binding site.* Biochemistry, 2011. **50**(48): p. 10559-65.
39. Norris, A.L. and E.H. Serpersu, *Antibiotic selection by the promiscuous aminoglycoside acetyltransferase-(3)-IIIb is thermodynamically achieved through the control of solvent rearrangement.* Biochemistry, 2011. **50**(43): p. 9309-17.
40. Norris, A.L., et al., *Protein dynamics are influenced by the order of ligand binding to an antibiotic resistance enzyme.* Biochemistry, 2014. **53**(1): p. 30-8.
41. Norris, A.L. and E.H. Serpersu, *Interactions of coenzyme A with the aminoglycoside acetyltransferase (3)-IIIb and thermodynamics of a ternary system.* Biochemistry, 2010. **49**(19): p. 4036-42.
42. Lewis Kay E., P.K., Tim Saarinen, *Pure absorption gradient enhanced heteronuclear single quantum correlation spectroscopy with improved sensitivity.* J. Am. Chem. Soc, 1992. **114**(26): p. 10663-10665.
43. Delaglio, F., et al., *NMRPipe: a multidimensional spectral processing system based on UNIX pipes.* J Biomol NMR, 1995. **6**(3): p. 277-93.
44. Schuck, P., *Size-distribution analysis of macromolecules by sedimentation velocity ultracentrifugation and lamm equation modeling.* Biophys J, 2000. **78**(3): p. 1606-19.
45. Schuck, P., *On the analysis of protein self-association by sedimentation velocity analytical ultracentrifugation.* Anal Biochem, 2003. **320**(1): p. 104-24.
46. Houtman, J.C., et al., *Studying multisite binary and ternary protein interactions by global analysis of isothermal titration calorimetry data in SEDPHAT: application to adaptor protein complexes in cell signaling.* Protein Sci, 2007. **16**(1): p. 30-42.
47. Keller, S., et al., *High-precision isothermal titration calorimetry with automated peak-shape analysis.* Anal Chem, 2012. **84**(11): p. 5066-73.
48. Serpersu, E.H., C. Ozen, and E. Wright, *Studies of enzymes that cause resistance to aminoglycosides antibiotics.* Methods in molecular medicine, 2008. **142**: p. 261-71.
49. Cooper, A., *Thermodynamic analysis of biomolecular interactions.* Curr Opin Chem Biol, 1999. **3**(5): p. 557-63.
50. Norris, A.L., C. Ozen, and E.H. Serpersu, *Thermodynamics and kinetics of association of antibiotics with the aminoglycoside acetyltransferase (3)-IIIb, a resistance-causing enzyme.* Biochemistry, 2010. **49**(19): p. 4027-35.

51. Ramirez, M.S. and M.E. Tolmasky, *Aminoglycoside modifying enzymes.* Drug Resist Updat, 2010. **13**(6): p. 151-71.
52. Garrett, R.H.a.G., C.M., *Biochemistry*. 2nd edition ed. 1999: Sanders College Publishing.
53. Wright, E. and E.H. Serpersu, *Enzyme-substrate interactions with an antibiotic resistance enzyme: aminoglycoside nucleotidyltransferase(2'')-Ia characterized by kinetic and thermodynamic methods.* Biochemistry, 2005. **44**(34): p. 11581-91.

Vita:

Sherin R. Raval was born in the city of Ahmedabad located in the state of Gujarat in the sub-continent of India. She moved to the United States in 2004 and completed her Bachelor's degree in Chemistry with a minor in Math from Indiana University South Bend (IUSB). Her interest in biochemistry was sparked while working with a metalloprotein, arsenite oxidase that detoxifies arsenite by converting it to arsenate in a soil bacterium, in the laboratory of Professor Gretchen L. Anderson at IUSB. Upon completion of her undergraduate degree, she started working as a Research Chemist for r^2 Diagnostics, Inc., a biotech firm in South Bend, IN. After working four years in the biotech industry she wanted to pursue her graduate education. In January 2011, she joined the Biochemistry and Cellular and Molecular Biology program at The University of Tennessee, Knoxville. In Dr. Engin H. Serpersu's laboratory, she worked on the issue of antibiotic resistance due to aminoglycoside modifying enzymes. Upon graduation she wishes to join a research group that fulfills her passion for drug discovery in health care.